AD-A035 865 VOUGHT CORP ADVANCED TECHNOLOGY CENTER INC DALLAS TEX F/G 20/4
HYDRODYNAMIC DRAG OF DISKS WITH COMPLIANT MEMBRANE/SUBSTRATE FA--ETC(U)
JAN 77 T D REED N00014-69-C-0214
UNCLASSIFIED ATC-B-94300/7CR-1 NL

1 OF 1
ADA035865

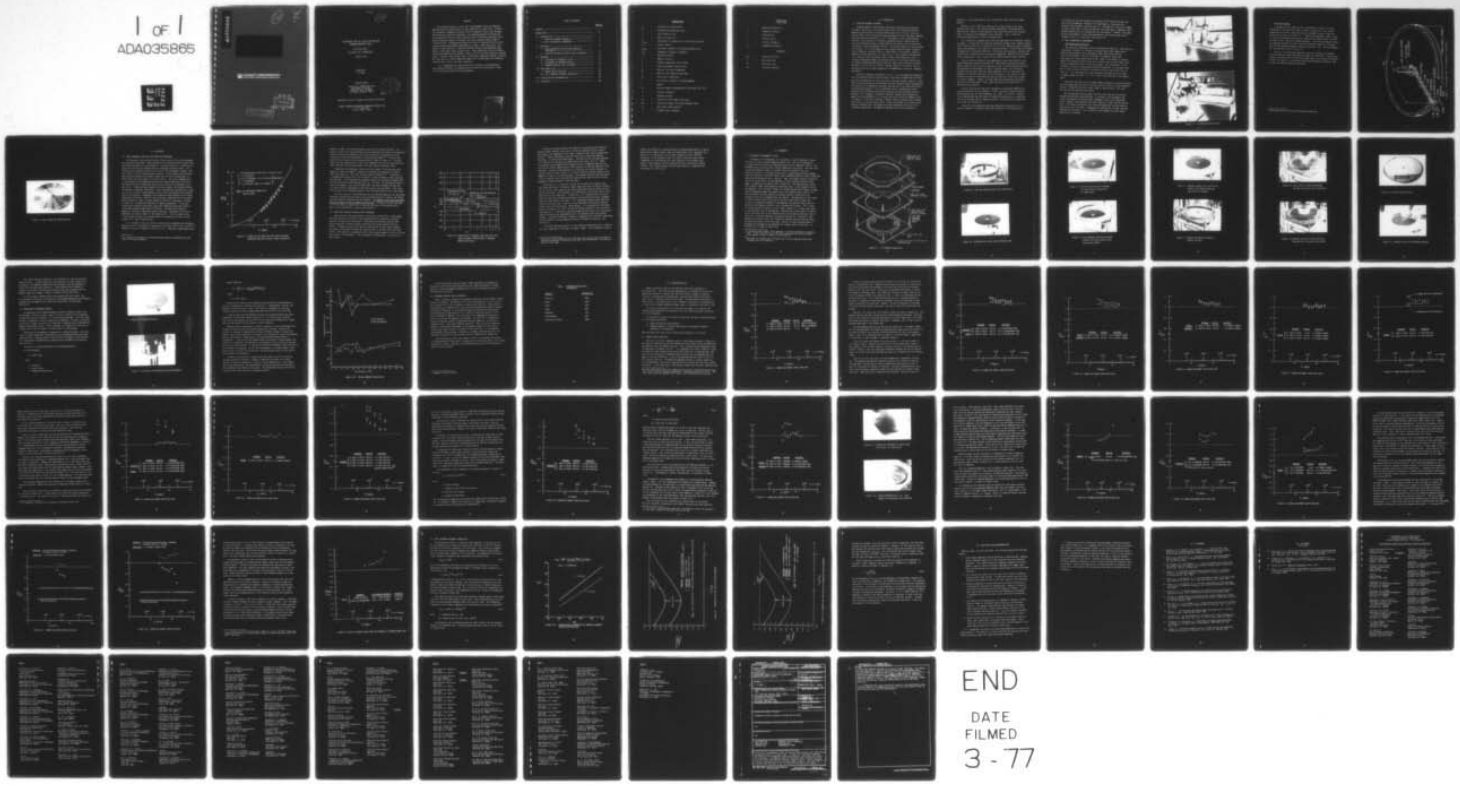

END

DATE
FILMED
3-77

12

8

VOUGHT CORPORATION
Advanced Technology Center, Inc.

(12)

HYDRODYNAMIC DRAG OF DISKS WITH COMPLIANT MEMBRANE/SUBSTRATE FACES

Technical Report

ATC Report No. B-94300/7CR-1

January 1977

Prepared by

T. D. Reed

Prepared Under

Contract No. N00014-69-C-0214
Department of the Navy
Office of Naval Research
Arlington, Virginia 22217

Approved for public release; distribution unlimited.

VOUGHT CORPORATION ADVANCED TECHNOLOGY CENTER, INC.
P. O. Box 6144
Dallas, Texas 75222

ABSTRACT

The rotational drag of a disk, with interchangeable faces of compliant membrane/substrate combinations, has been measured in a water tank. A device for stretching a membrane uniformly and with repeatable results was designed, fabricated and successfully employed. Six membrane materials and three substrate materials were utilized to fabricate over 36 different compliant disks. Each of these was tested in turbulent flow over a Reynolds number range of $1.77\text{-}2.95 \times 10^6$. A maximum drag reduction of 19% is indicated from tests with a heavy polyurethane membrane unbonded to an organic rubber substrate. This amount of drag reduction is inferred from data taken with polyurethane sheet material which had a rough surface finish. Thus, additional tests with smooth polyurethane membranes are needed in order to verify the drag reductions reported herein. However, these results tend to follow Ash's membrane frequency criterion. But other data for similar membranes suggest this criterion may be a necessary condition but is not a sufficient condition.

It is recommended that future exploratory studies of the hydrodynamic drag reduction potential of membrane walls be done with flat plates in order to facilitate more detailed flow measurements.

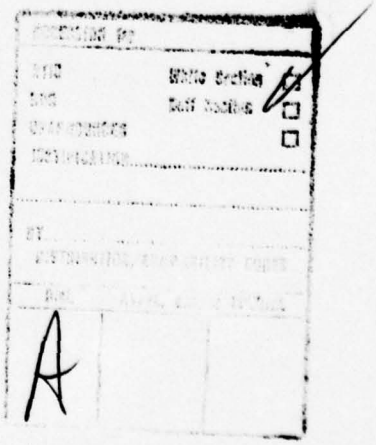

TABLE OF CONTENTS

	Page No.
ABSTRACT	1
NOMENCLATURE	iii
1.0 INTRODUCTION	1
1.1 COMPLIANT BOUNDARY RESEARCH	1
1.2 BASIC EXPERIMENTAL ARRANGEMENT	3
2.0 SUBSTRATES	8
2.1 HARD, REFERENCE DISKS AND DATA REDUCTION PROCEDURE	8
2.2 COMPLIANT SUBSTRATE MATERIALS AND THICKNESSES	10
3.0 MEMBRANES	14
3.1 ATTACHMENT OF MEMBRANES TO DISK	14
3.2 MEASUREMENT OF MEMBRANE TENSION	21
3.3 MEMBRANE MATERIALS AND THICKNESSES	25
4.0 EXPERIMENTAL DATA	27
4.1 MOMENT COEFFICIENT DATA	27
4.2 ASH'S MEMBRANE FREQUENCY CORRELATION	53
5.0 CONCLUSIONS AND RECOMMENDATIONS	58
6.0 REFERENCES	60

NOMENCLATURE

A	-	Amplitude of surface motion
A^+	-	Nondimensional amplitude, AU_τ/ν
a	-	Outer radius of disk
b	-	Radius of center hub
$C_{F_{avg}}$	-	Coefficient of average skin friction acting on disk
E	-	Young's modulus
F_{peak}	-	Peak power frequency of turbulent boundary layer
F_{vib}	-	Fundamental frequency of membrane
h	-	Membrane thickness
I	-	Moment of inertia
ℓ	-	Length of cantilever (drive shaft)
M	-	Total drag moment acting on disk
M_m	-	Mass per unit area of membrane
m	-	Mass per unit length of cantilever
m_c	-	Total mass of cantilever
P	-	Gas pressure applied to inflate membrane
r	-	Radius
Re	-	Reynolds number corresponding to disk conditions, $a^2\omega/\nu$
S	-	Flexural stiffness
T	-	Membrane tension
U_e	-	Velocity at outer edge of disk (ωa)
U_∞	-	Velocity at edge of flat plate boundary layer
U_τ	-	Wall shear stress velocity
δ	-	Boundary layer thickness

NOMENCLATURE
(Continued)

η	-	Membrane deflection at r
ν	-	Kinematic viscosity
ρ	-	Fluid density
σ	-	Poisson's ratio
ω	-	Circular frequency
ω_1	-	Fundamental frequency

SUBSCRIPTS

abs	-	Asbestos substrate
e	-	Edge conditions
HD	-	Hard disk value
sty	-	Styrofoam substrate

1.0 INTRODUCTION

1.1 COMPLIANT BOUNDARY RESEARCH

Although numerous investigations have been conducted during the past ten years, there are still no established criteria for designing compliant boundaries which reduce turbulent boundary layer skin friction. No satisfactory theory exists, and conflicting experimental results have been reported. As noted recently by Bushnell, et al.[1], the problem is not straightforward. "The walls are exposed to a relatively wide-band spectral loading and the structural dynamics problem is complicated by the necessity of including the influence of induced aerodynamic forces. The prime variables are multitudinous and include: (a) flow parameters such as speed, Reynolds number, boundary layer thickness, and state (laminar, transitional, or turbulent), pressure gradient and flow medium (air or water, etc.); (b) structural configuration, i.e., vertical and/or horizontal layers, two or three dimensions, with or without pretensioned members and the possibility of non-linear effects such as caused by membranes backed with small air gaps; and (c) material property parameters such as density, modulus, damping, degree of anisotropy, and the possible variation of these properties with temperature, vibration, frequency, and aging."

The basic hypothesis of Bushnell, et al.[1], as to how compliant boundaries could conceivably reduce turbulent shear stress, may be summarized as follows. Previous investigations of the structure of turbulent boundary layers on rigid walls have established the existence of bursting frequencies which characterize the ejection of low momentum fluid away from the wall, e.g. Offen and Kline,[2] Strickland and Simpson.[3] This low momentum fluid is replaced with higher momentum fluid coming from upstream of the burst and moving toward the wall. Bushnell, et al. suggest a successful compliant boundary would modulate or damp the burst phenomena so as to reduce the rate at which low momentum fluid is ejected. If this were affected, a smaller velocity gradient and a reduced shear stress at the wall would result. These investigators also believe this requires surfaces which can respond with high frequencies and low ($A^+ < 6$) to moderate amplitudes. Mathematical modeling of this burst modulation

hypothesis is being performed by Prof. Orszag (MIT) under contract to NASA Langley.

Bushnell, et al.[1] have also conducted a critical review of all known compliant wall data. This review discusses experimental investigations of compliant wall effects on both boundary layer transition and fully turbulent flows. An extensive bibliography is also included. Thus, a review of nonrotating experiments will not be repeated here.

R. N. Brown[4] has conducted noise and drag experiments with compliant rotating cylinders. In these tests at the Naval Underwater Systems Center, Newport Laboratory, 0.159 cm (1/16 in.) to 0.635 cm (1/4 in.) thick rubber and other viscoelastic layers were attached to the side of an aluminum cylinder. The cylinder was rotated at speeds up to 30.5 m/sec (100 fps). Fluctuating wall pressures, cylinder wall accelerations, radiated noise, and drag were measured. Beyond a critical speed, drag increases occur, but no cases of drag reduction have yet been reported.

The only previous compliant disk experiments, that we are aware of, are those conducted by Hansen and Hunston.[5,6] These authors measured the hydrodynamic drag of disks with 1/3 cm coatings of 10, 15, 20 and 25% PVC plastisol. They observed the development of radial, standing waves in the compliant surfaces when the disk rotational speed exceeded a critical value that was dependent on the shear modulus of the surface coating. An increase in drag followed the onset of these waves and was ascribed to an effective increase in surface roughness. However, no drag reduction was measured, even before the onset of surface waves. Thus, these tests were also unsuccessful in achieving drag reduction.

The ATC rotating disk tests were designed to investigate membrane-substrate combinations for two reasons. Firstly, previously reported cases of drag reduction have utilized membranes, e.g., Refs. 7, 8, and 9. Secondly, it was hypothesized that the onset of standing surface waves on a compliant disk could be controlled via membrane tension. The test results proved this to be true, see Section 3.3.

Selection of the membrane-substrate combinations was guided by (1) a review of materials reported to have been successful in previous tests of

flat plates and (2) the frequency correlation of Ash[10] which indicates the ratio of the fundamental frequency of the membrane to a characteristic turbulent flow frequency should be near 1/2. Although this correlation seemed to provide some order to previous compliant flat plate data, independent tests at NASA Langley failed to substantiate this correlation.[1] However, the lowest ATC disk drag appears to have been obtained with the lowest value of this frequency ratio (i.e., near one), see Section 4.2.

1.2 BASIC EXPERIMENTAL ARRANGEMENT

ATC Rotating Disk Facility

The tests were conducted in the ATC Rotating Disk Facility. This facility, illustrated in Figure 1-1, consists of a motor driven shaft supported by bearings and extending into a rectangular tank 165 cm long, 95.3 cm wide, and 65 cm deep. The top of the tank is hinged for access and seals against a rubber gasket when closed. Power is provided by a constant speed 7.5 horsepower electric motor with a belt driven, variable speed transmission connecting the motor to the drive shaft. The transmission is continuously variable in output speed from 500 to 5000 rpm. A right-angle gear box is used in the drive shaft to provide a vertical rotation axis for the facility. Two right-angle units are available to provide ratios of input to output speeds of either 1:1 or 2:1. The 2:1 unit was used in the subject tests.

Variable reluctance (no slip rings) torque transducers are mounted beneath the right-angle gear box and in-line with the drive shaft to directly measure torque. Transducers with full scale ranges of 100 and 500 in. lbs. were utilized for the compliant disk tests.

At the beginning of these tests the drive shaft bearings consisted of two water-lubricated, nylon bushings. In the past, this arrangement had proven satisfactory for testing small (diameters <28 cm) and lightweight disks. However, the compliant disk tests required a larger and much heavier disk. Preliminary testing with this disk indicated metal bearings would be required to carry the loads. Subsequently, a matched set of super precision bearings were installed. This resulted in much smoother and more stable operation at all speeds.

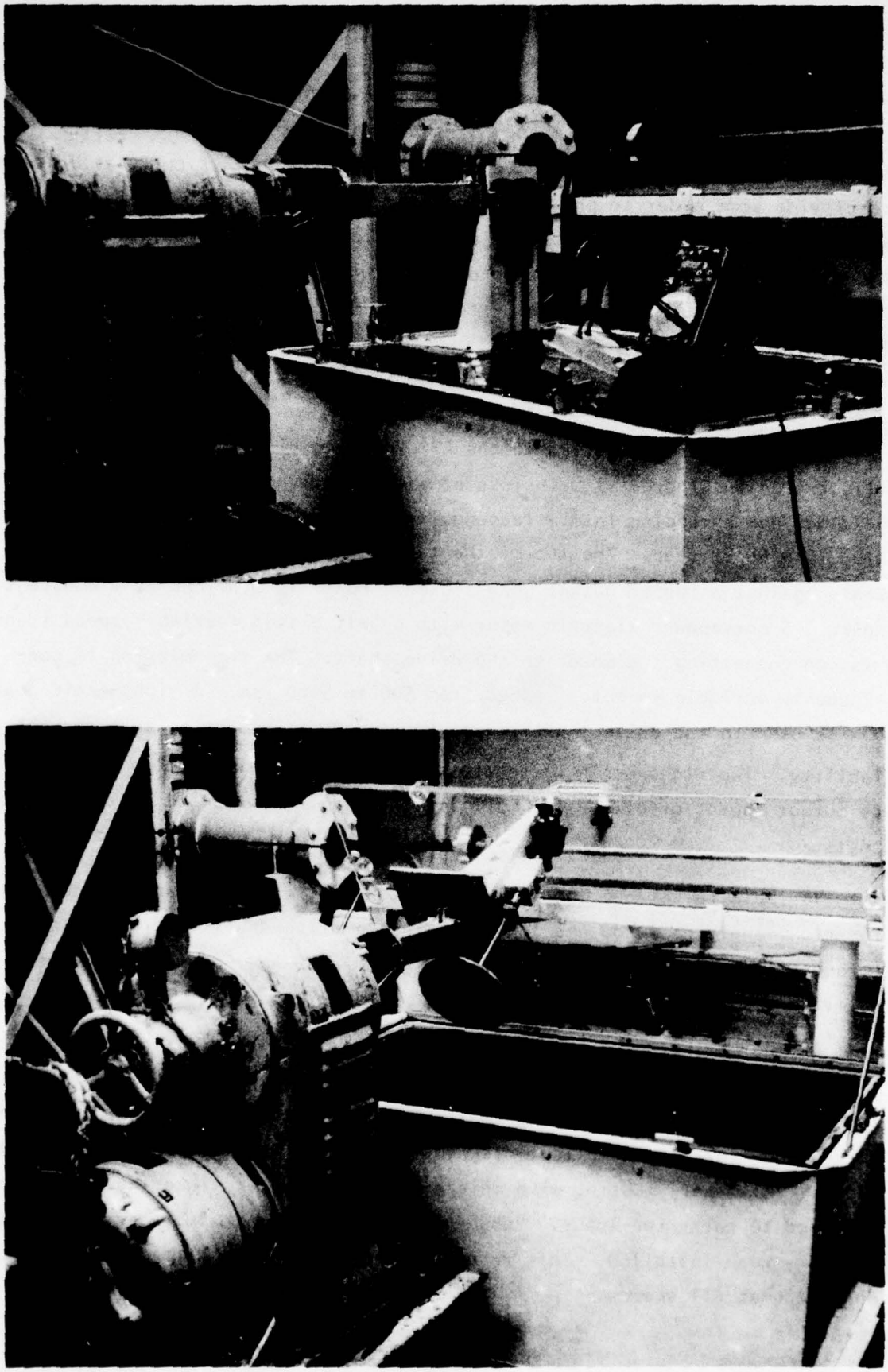

FIGURE 1-1. ATC ROTATING DISK FACILITY

Basic Disk Design

A schematic of the compliant disk is presented in Figure 1-2, and a photograph of the basic disk frame is shown in Figure 1-3. The relevant dimensions of the disk, substrate cavities, membrane retainer rings, and center hub are given in Figure 1-2. It should be noted that a total of four O-rings are used beneath the retainer rings and the center washers in order to obtain an air tight seal beneath membranes. This feature along with three gas passages through the side of the disk* provided a means for inflating the disk and measuring membrane tension (see Section 3.2). The gas passages are indicated by arrows in Figure 1-3.

The disk, with Plexiglas substrates, was spin balanced on a Noremac Vibration Analyzer (Model VAS-1200) at speeds up to 1400 rpm. A satisfactory balance was achieved by drilling three holes normal to the plane of the disk. As shown in Figure 1-3, these holes were located beneath the retainer rings so that the external shape was unaltered.

*Three holes were drilled to facilitate spin balancing.

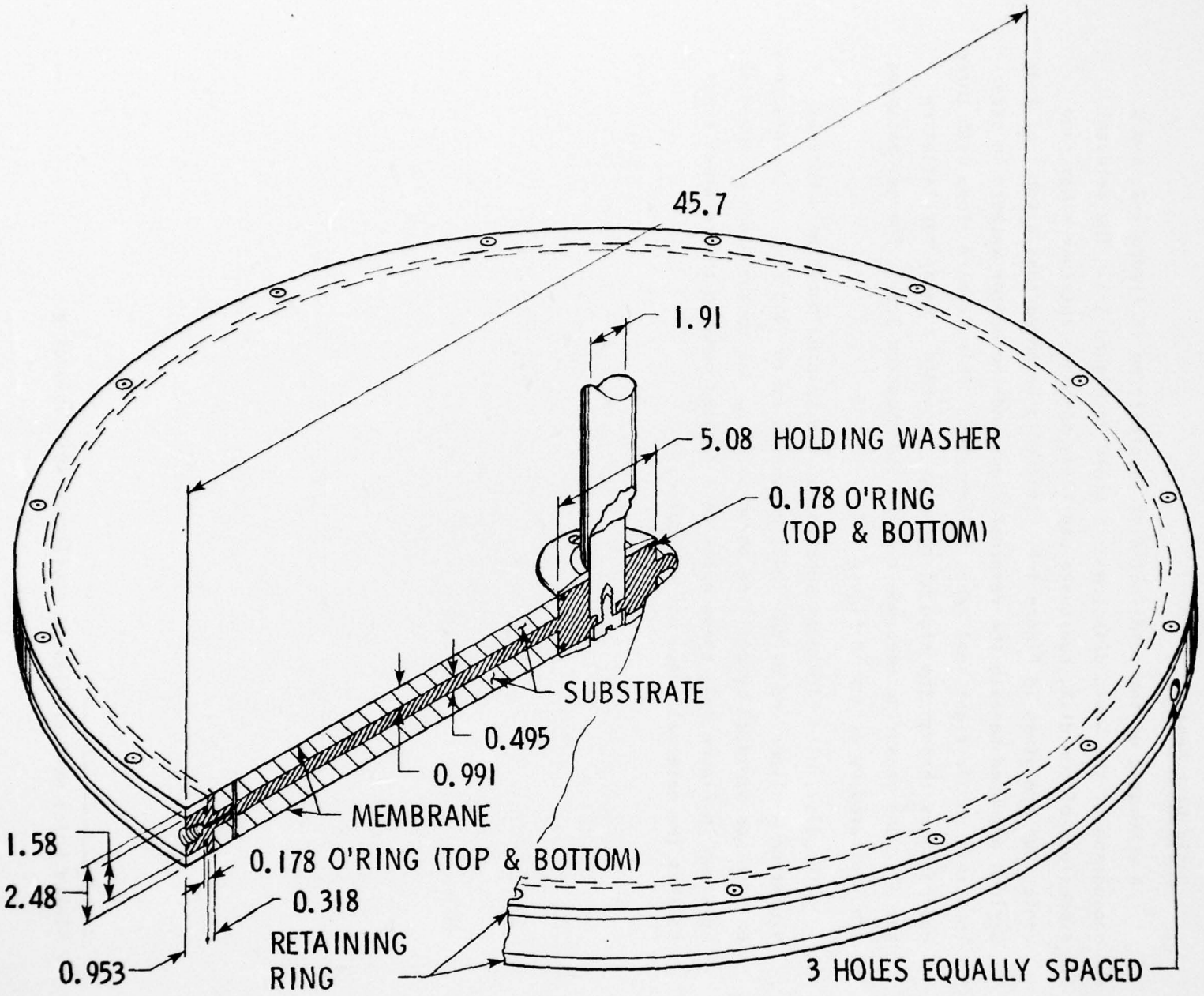

FIGURE 1-2. ATC COMPLIANT DISK (ALL DIMENSIONS IN CENTIMETERS)

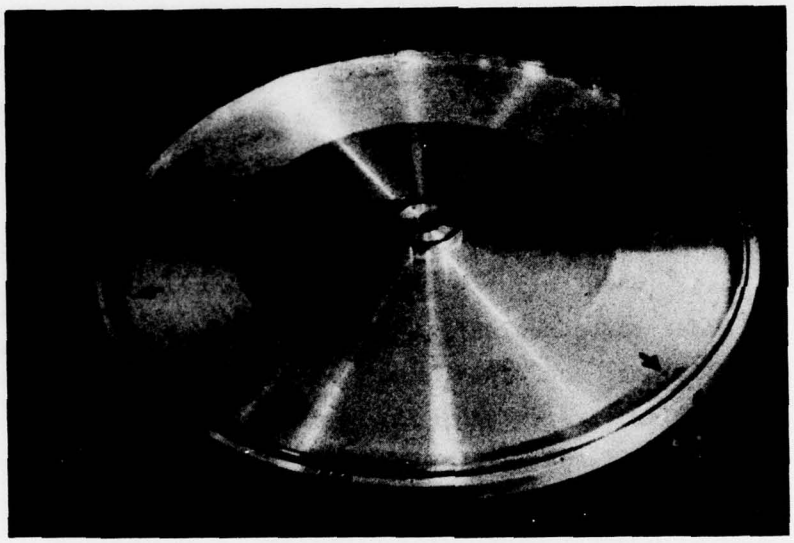

FIGURE 1-3 BASIC FRAME FOR COMPLIANT DISKS

2.0 SUBSTRATES

2.1 HARD, REFERENCE DISKS AND DATA REDUCTION PROCEDURES

As discussed in the previous section, the disk was initially spin balanced with Plexiglas substrates. These substrates were covered with 2 mil Mylar which was bonded to them with a spray adhesive. The resulting disk was tested in the water tank and provided reference data for subsequent compliant disks. This procedure was followed during the first half of the experimental program. However, after a period of approximately 6 months, it was observed that the Plexiglas substrates warped and creeped; enough that they had to be put back in a lathe before they would again fit the disk cavity. After this happened twice, it was decided to use something that would not require additional lathe work. Two additional sets of Plexiglas inserts were on hand with thicknesses of 1/2 and 1/3 cm. (These had been designed to serve as spacers for testing different thicknesses of compliant substrates.) Since styrofoam was available and is easy to cut with a hot wire, approximately 2/3 cm inserts were made to place beneath the 1/3 cm Plexiglas. Subsequent tests showed the drag (torque) of the lighter weight disk to be less. When this was discovered, substrates of all styrofoam were fabricated in order to reduce weight of the disk to a minimum. As shown in Figure 2-1, no additional decrease in torque was measured.* It was concluded that the heavier substrates caused more imbalance during spin which in turn produced greater amplitudes of vibration. The additional vibration apparently resulted in additional drag on the disk. The possibility of this phenomenon was noted by Kempf in 1922 (Goldstein[11]). With this observation, it was decided to adopt the styrofoam disks, with bonded 2 mil Mylar, as the standard for a hard, reference disk.

It is relevant to note the initial, hard disk data, obtained with Plexiglas, agreed well with a semi-empirical estimate of the total drag of a 45.7 cm (18 in.) diameter disk with a thickness of 2.54 cm (1 in.). These early measurements were

---

*This study of the effects of varying substrate weight was conducted with the 100 in-lb torque transducer.

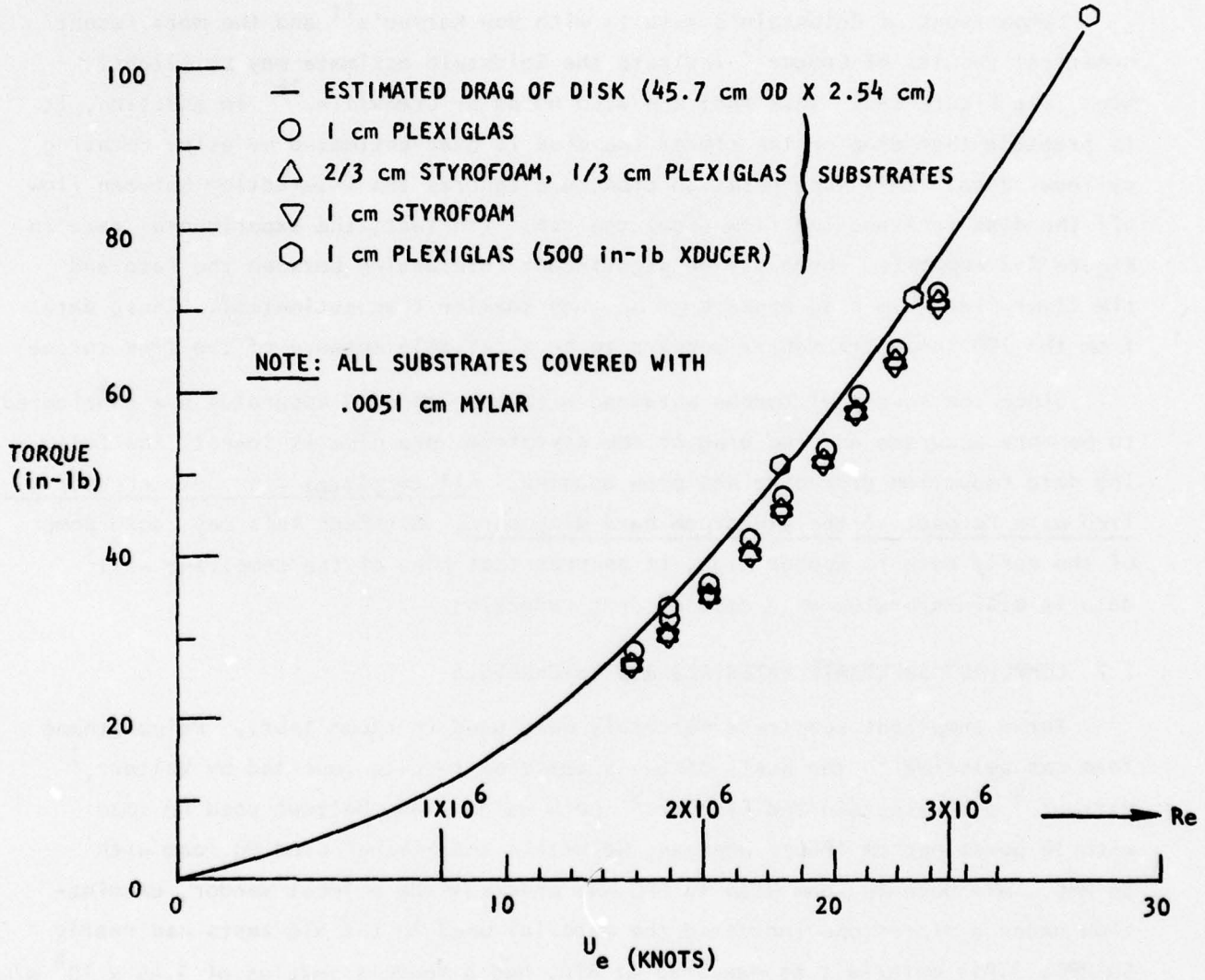

FIGURE 2-1. TORQUE DATA FOR HARD DISK WITH THREE DIFFERENT SUBSTRATES AND TWO DIFFERENT TORQUE TRANSDUCERS

made with a 500 in-lb torque transducer and nylon drive shaft bearings. The drag on a "thin" disk was estimated using the semi-empirical results of Goldstein,[11] and the contribution produced by the finite thickness was estimated from the rotating cylinder drag correlation of Theodorsen and Regier.[12] A typical comparison of this data with the estimated drag is shown in Figure 2-1. Interestingly, the data obtained with a 100 in-lb transducer and a set of super precision shaft bearings indicate approximately 10% lower drag for Plexiglas disks.

Comparisons of Goldstein's results with Von Karman's[11] and the more recent numerical results of Cooper[13] indicate the Goldstein estimate may be slightly high, see Figure 2-2. This fact was also noted by Granville.[14] In addition, it is probable that drag on the rim of the disk is over-estimated by using rotating cylinder data. This superposition procedure ignores the interaction between flow off the disk face and the flow about the rim. (In fact, the experimental data in Figure 2-2 suggests there may be significant interaction between the face and rim flows since rim drag appears to be much smaller than estimated). Thus, data from the 100 in-lb transducer appears to be a reliable measure of the true torque.

Since the levels of torque obtained with the improved apparatus are considered to be more accurate and the drag of the styrofoam hard disk is lowest, the following data reduction procedure has been adopted. All compliant disk data are normalized with respect to the styrofoam hard disk data. Although this may cause some of the early data to appear high, it assures that none of the compliant wall data is misinterpreted as a case of drag reduction.

2.2 COMPLIANT SUBSTRATE MATERIALS AND THICKNESSES

Three compliant substrate materials were used in these tests. Polyurethane foam was selected on the basis of the successful results reported by Walters,[7] Mattout,[8] and Weinstein and Fischer.[9] Both Walters and Mattout used PU foam with 16 pores per cm (PPC); whereas, Weinstein and Fischer used PU foam with 39 PPC. Although PU foam with 16 PPC was ordered from a local vendor, examination under a microscope indicated the material used in the ATC tests had nearly 50 PPC. This material, as measured at ATC, had a Young's modulus of 3.45×10^4 N/m and a density of 0.029 gm/cc. Two thicknesses of approximately 1 cm and 1/3 cm were tested.

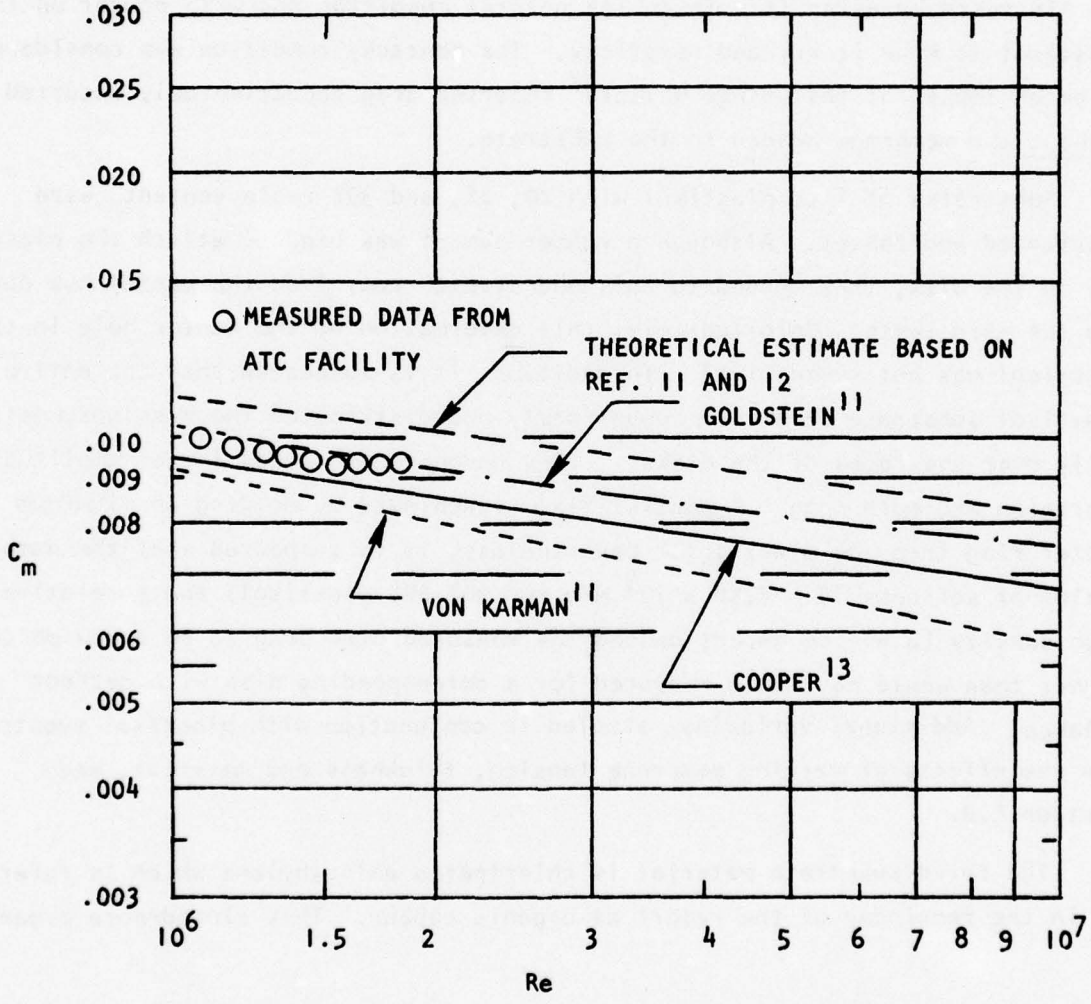

FIGURE 2-2. COMPARISON OF STYROFOAM, HARD DISK DATA WITH THREE DIFFERENT CORRELATIONS OF TURBULENT MOMENT COEFFICIENT

Polyvinyl chloride plastisol was chosen as a second substrate material because Young's modulus can be easily varied by changing the resin content. This material was apparently first used in compliant wall tests by Hansen and Hunston.[5] These investigators used PVC plastisols, without any membrane coverings, in rotating disk experiments. The material has also been employed as a substrate on flat plates at NASA Langley by Fischer, et al.[15] These investigators used 0.0025 cm-thick sheets of Mylar as membrane material and utilized the natural adhesiveness of PVC plastisol to hold the membrane to the substrate. The use of PVC plastisol as a substrate was further explored in the ATC tests by using it both in its natural condition and with powder on the plastisol to make it dry and nonsticky. The nontacky condition was considered to be an important test since Walters[7] reported drag reduction only occurred without the membrane bonded to the substrate.

Substrates of 1 cm plastisol with 20, 25, and 30% resin content, were fabricated and tested. Although a rubber cement was used to attach the plastisol to the disk, they tended to pull and stretch away from the center hub during the spin tests. Unfortunately, this deformation of the center hole in the plastisol was not symmetrical. In addition, it is suspected that the entire plastisol substrate stretched nonuniformly and distributed the mass unsymmetrically over the faces of the disks.* This undoubtedly caused larger amplitude vibration and more drag. A partial fix was achieved by molding an aluminum center ring into the plastisol. Nevertheless, it is suspected that the combination of softness ($E = 7.58 \times 10^3$ N/m for 20% PVC plastisol) and a relatively high density ($\rho = 1.06$ gm/cc) caused the measured disk drag to be a few percent higher than would have been measured for a corresponding disk with perfect balance. Additional variables, studied in conjunction with plastisol substrates, are the effects of varying membrane tension, thickness and material, see Section 4.0.

The third substrate material is chlorinated polyethylene which is referred to in the remainder of the report as organic rubber. This closed-pore organic

*PVC plastisol substrates with less than 20% resin content were not feasible because of excessive stretching at the center hub and humping of the material near the outer edge.

rubber was selected as a candidate material because theoretically it can be molded with a smooth surface, does not absorb water, has a relatively low density (ρ = 0.246 gm/cc), and a Young's modulus of 2.45×10^5 N/m^2. Originally, it was planned to test this material both with and without a membrane, but unfortunately the local supplier of this material was unable to mold samples with the required size and a sufficiently smooth surface. Thus, organic rubber was used exclusively as a substrate with thicknesses of 1 and 1/3 cm.

3.0 MEMBRANES

3.1 ATTACHMENT OF MEMBRANES TO DISK

A schematic of the apparatus for stretching a circular membrane is shown in Figure 3-1 and is labeled membrane tension rig. The rig is designed to (1) apply uniform tension to a membrane and (2) enable repeatable results. The procedure used in constructing a typical membrane is as follows. The disk, with a substrate bonded in place, is placed inside the stretcher ring, see Figures 3-2 and 3-3. The depth of the cavity is approximately 0.05 cm greater than the thickness of the disk frame so that a membrane does not usually touch the substrate during application of tension.* Next, the support plate is placed on top of the corner bolts, and the membrane, with bar weights attached to the edges, is placed on the support plate, Figure 3-4. The clamping plate, which has a nonskid rubber sheet bonded to the bottom side, is then placed on top of the membrane. Four to eight C-clamps are attached around the periphery to sandwich the membrane between the support plate and clamping plate, Figure 3-5.** The bar weights are then removed, and primary tension is applied by the stretcher ring as the clamped plates are lowered. The magnitude of the tension is controlled by height of the nuts on the four corner bolts, Figure 3-6. In order to complete attachment of the membrane, the applied tension must be held while the membrane retainer ring is attached with screws. This is done by placing the entire tension rig in a press, Figure 3-7. A heavy cover plate is then placed on top of the membrane. The OD of this cover plate is sized to rest on the outer wall of the substrate cavity and allow the retainer ring to slide over it onto the membrane, see Figures 3-8 and 3-9. Pressure is then applied to the cover plate, the C-clamps are removed, and the retainer ring is attached with screws to the disk frame. Finally, a center holding washer is attached and the edges of the membrane are trimmed flush with the disk. A finished disk is shown in Figure 3-10.

---

*An exception occurs when a thick membrane is already attached to the bottom side. In this case the nuts on the corner bolts must be raised an appropriate amount in order to obtain a given tension.

**The number of C-clamps was increased from 4 to 8 as applied tension was increased from 125 to 800 N/m.

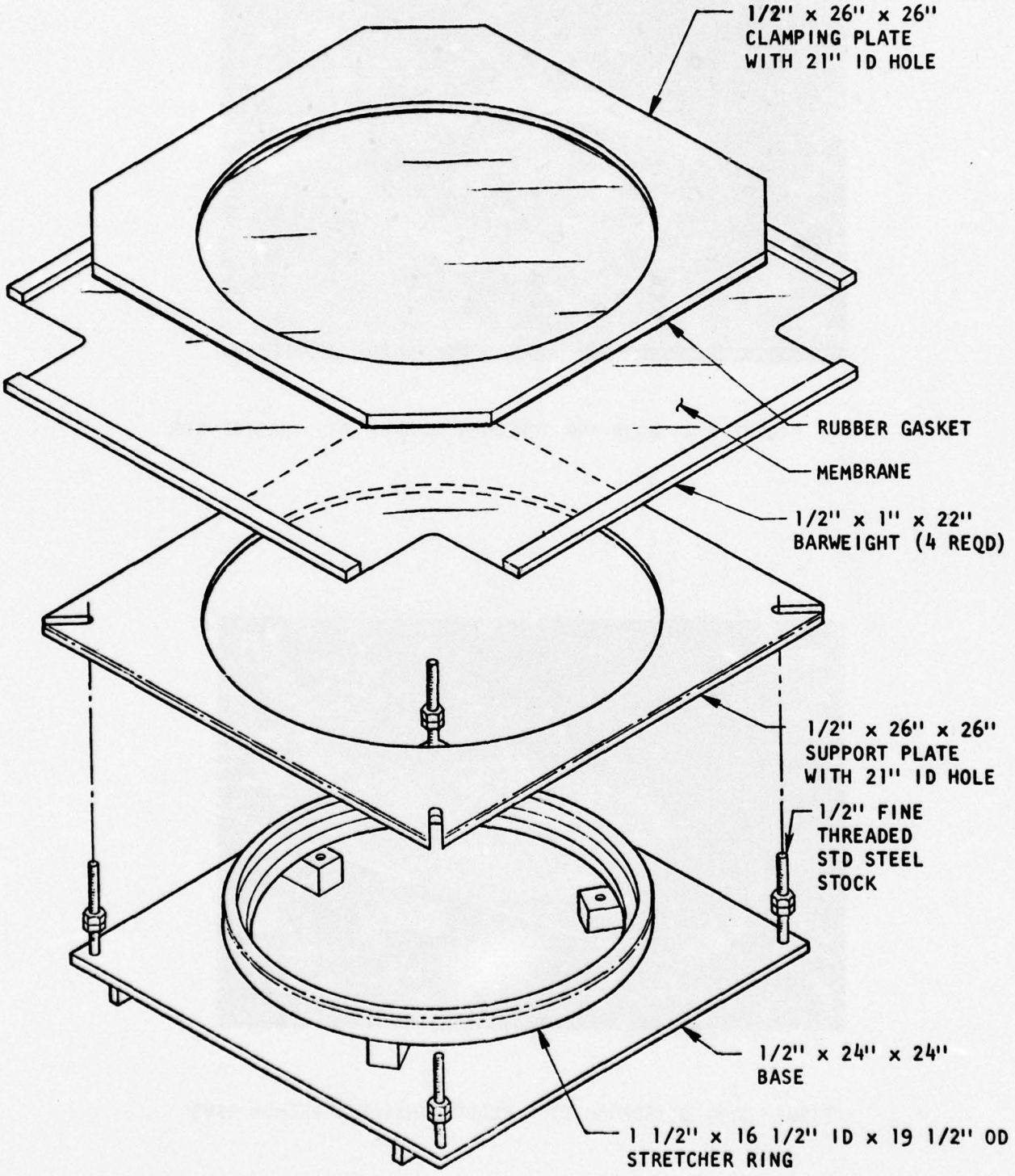

FIGURE 3-1. ATC MEMBRANE TENSION RIG

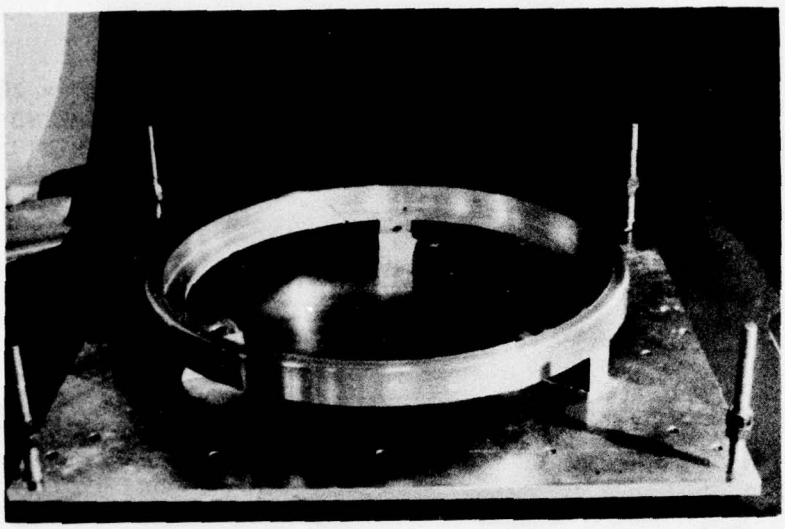

FIGURE 3-2. BASE AND STRECHER RING OF ATC TENSION RIG

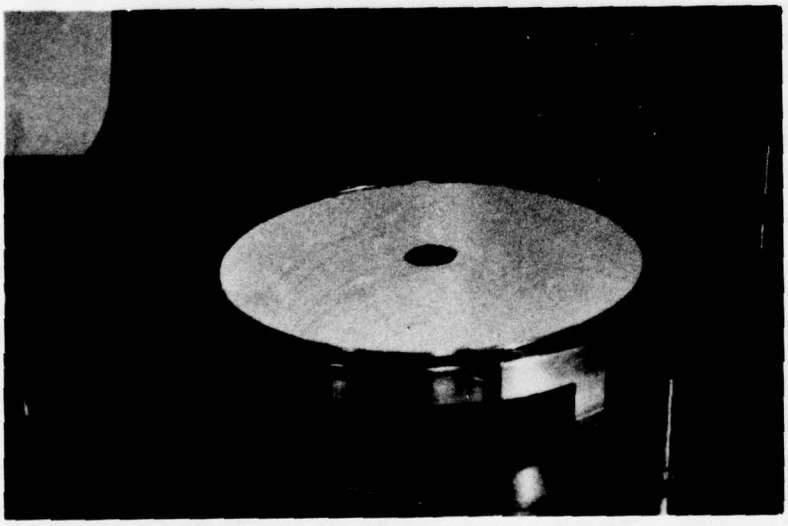

FIGURE 3-3. STYROFOAM DISK PLACED INSIDE STRECHER RING

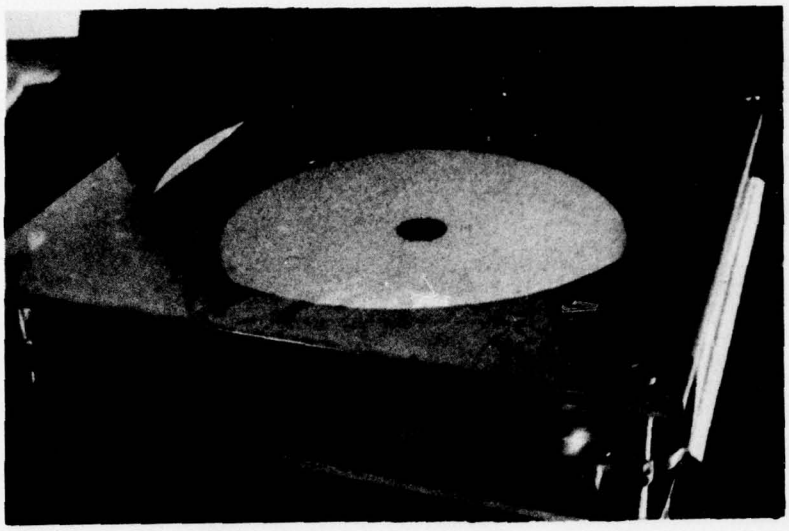

FIGURE 3-4. SUPPORT PLATE AND MYLAR MEMBRANE WITH BAR WEIGHTS PLACED ON TOP OF CORNER BOLTS

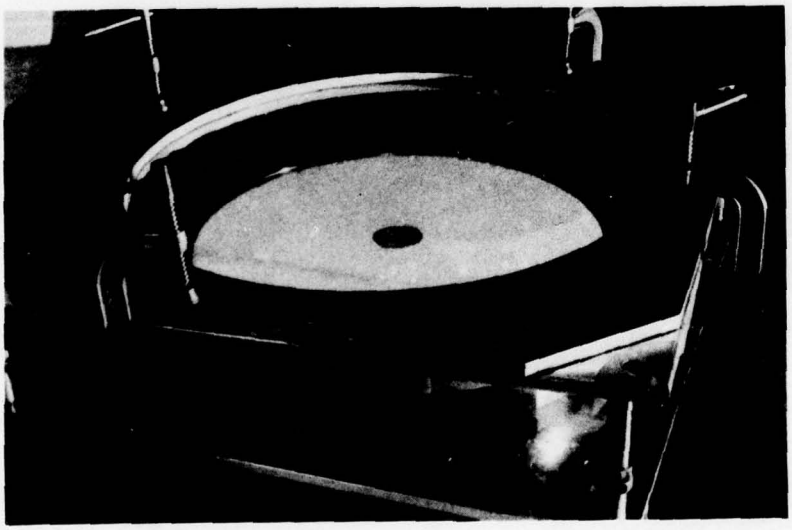

FIGURE 3-5. MYLAR MEMBRANE SANDWICHED BETWEEN SUPPORT PLATE AND CLAMPING PLATE, BAR WEIGHTS REMOVED

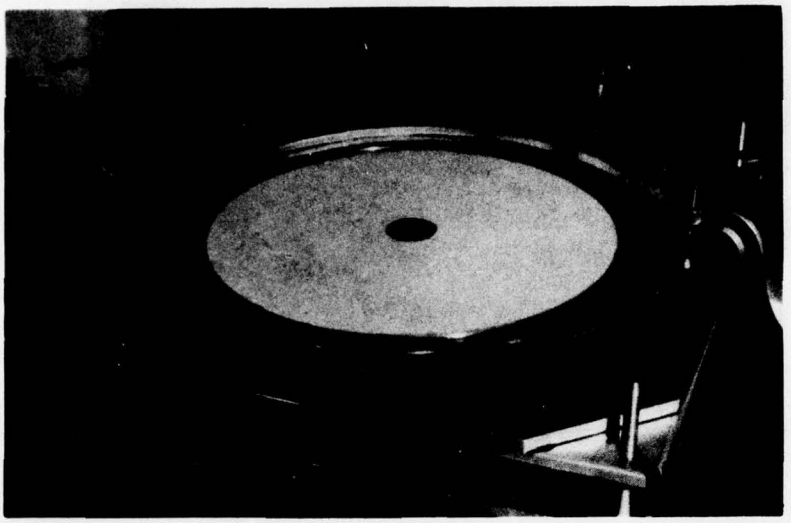

FIGURE 3-6. MEMBRANE LOWERED INTO POSITION FOR CONTACT WITH STRECHER RING AND APPLICATION OF TENSION

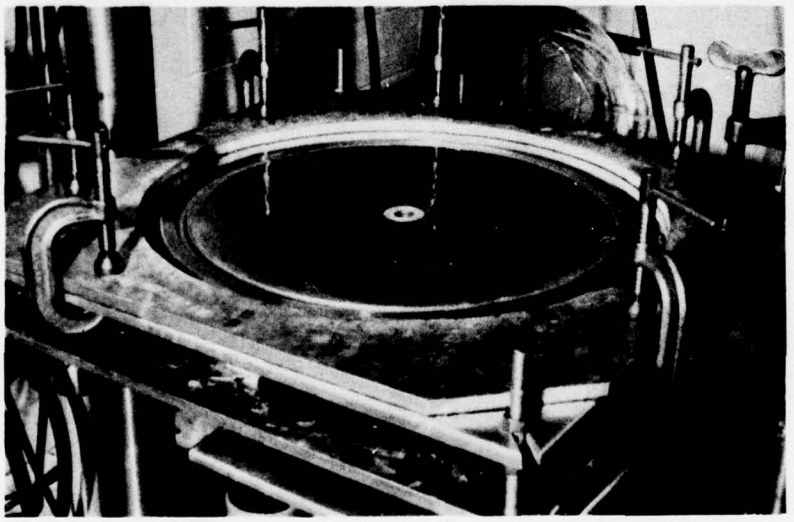

FIGURE 3- 7. COMPLETE TENSION RIG PLACED ON PEDESTAL OF PRESS

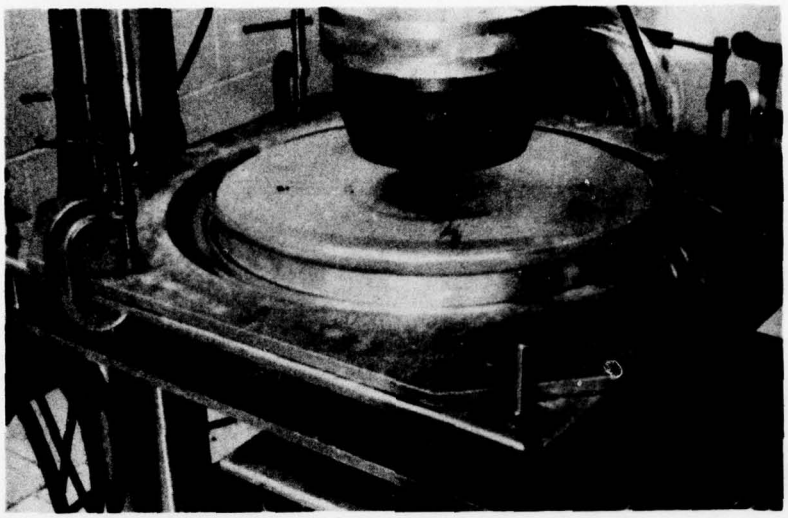

FIGURE 3-8. COVER PLATE IN PLACE AND MEMBRANE RETAINER RING RAISED FOR ILLUSTRATION

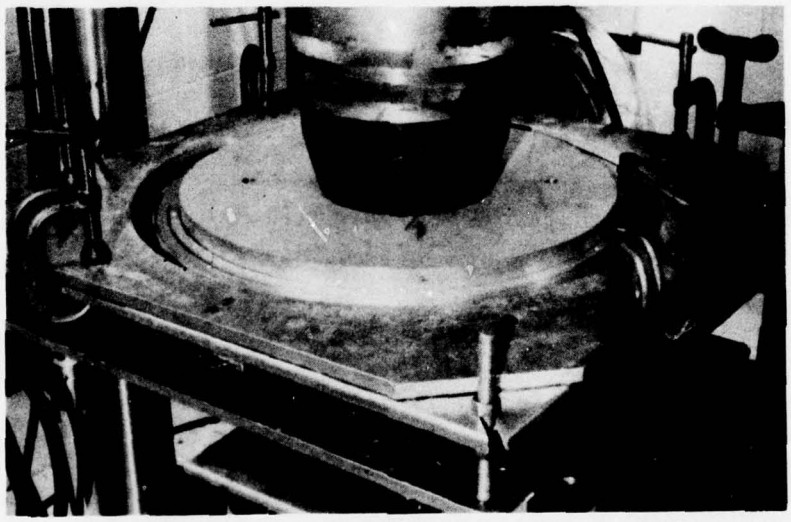

FIGURE 3- 9. PRESSURE APPLIED TO COVER PLATE WITH RETAINER RING IN PLACE BUT UNATTACHED

FIGURE 3-10. FINISHED COMPLIANT DISK

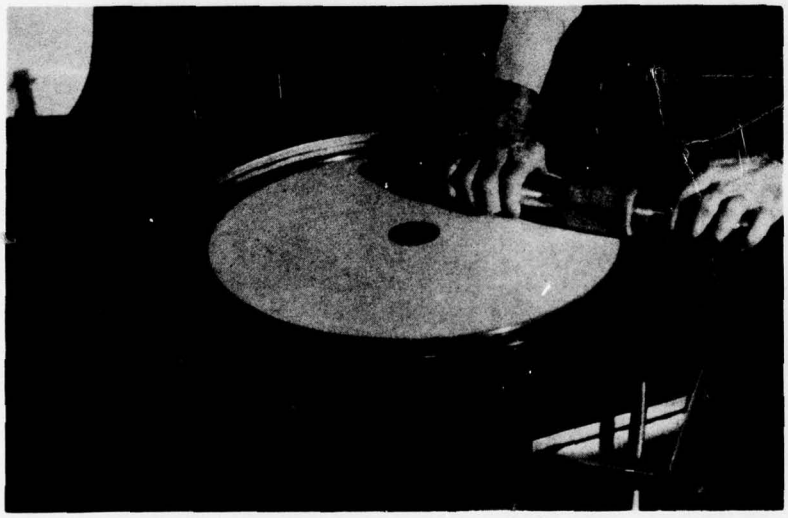

FIGURE 3-11. BONDING OF MYLAR TO STYROFOAM SUBSTRATE

This rather elaborate procedure is not necessary for constructing hard, reference disks. In these cases, the hard substrate is simply sprayed with an adhesive, the membrane lowered onto the stretcher ring, and subsequently rolled onto the substrate, Figure 3-11. After bonding, the C-clamps are removed, the retainer ring and center holding washer are attached, and the membrane edges are trimmed. Figure 3-12 shows a typical hard disk.

All of the hard, reference disks were covered with 2 mil Mylar. The only exception to this was in the case of polyurethane membranes where membrane roughness was suspected to be a significant contributor to disk drag, Section 4.0.

3.2 MEASUREMENT OF MEMBRANE TENSION

The apparatus used to measure membrane tension is shown in Figure 3-13. Gas passages in the disk frame, Figure 1-2, permit inflation of the membrane so that tension can be measured. In order to assure the gas is dry and clean, bottled nitrogen gas is used to pressurize the membrane. Pressure is typically varied over a range from 0.02 to 0.3 N/cm^2 and is measured with an MKS Baratron pressure measurement system. Since a membrane is on each side of the disk, a holding ring is used to support the disk around its outside edge.

Deflection of the membrane is measured via a 400x microscope. The microscope is simply focused on a reference point on the membrane before and after pressurization. Since the depth of focus of this instrument is less than one mil, measurements of deflection are conservatively estimated to be accurate within one mil.

The tension is then calculated by the following equations:

Circular Membrane

$$T = P(a^2-r^2)/4\eta$$

where

P = pressure
a = outer radius
η = membrane deflection at r

FIGURE 3- 12. FINISHED HARD DISK

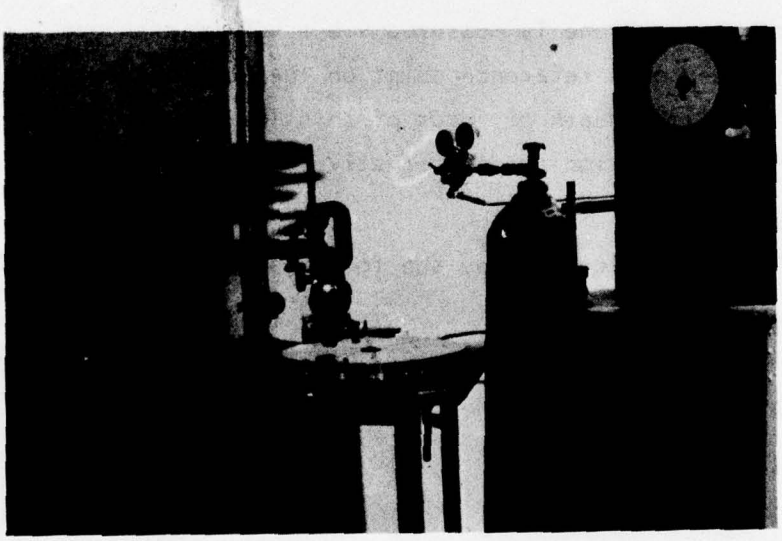

FIGURE 3- 13. APPARATUS FOR MEMBRANE TENSION MEASUREMENTS

Annular Membrane

$$T = P \left[(a^2 - r^2) + \frac{a^2 - b^2 \ln(r/a)}{\ln(a/b)} \right] / 4\eta$$

where

b = inner radius .

Uniformity of tension may be checked by making deflection measurements at various circumferential locations and values of r. Measurements indicate the tension is uniform to within ± 6%. With regard to repeatability, the data indicated tension variations between membranes can be held to less than 10%.

It may be noted that the membrane tension can be measured before and after attachment of the center washers (Figure 1-2). An initial check indicated that, within the accuracy of the data, the resulting annular membrane did indeed have the same tension as the original, circular membrane.

Membrane tension measurements, without a substrate, can be accomplished with minimum difficulty using this inflation-deflection technique. Typical data scatter for tensions of approximately 340 and 510 N/m are shown in Figure 3-14. However, when a Mylar membrane is in contact with substrates of either polyurethane foam or PVC plastisol, large scatter in the pressurized deflection data is encountered. In the case of polyurethane foam, electrostatic charge between foam and Mylar is suspected. Applications of an antistatic fluid to both the foam and Mylar did not seem to help. In the case of plastisol substrates, nonuniformities in the thickness is suspected. By the time the membrane is inflated enough to completely clear all parts of the plastisol, the gas pressure begins to add significant tension to the membrane.

In order to alleviate this problem and move forward with the testing over the desired range of tensions, a number of membranes were made with a given tension, without the substrates, in order to check repeatability. Once repeatability was ascertained, the same membrane stretching procedure was then used to place membranes over compliant substrates. The assumption being that flush substrates do not significantly alter membrane tension.

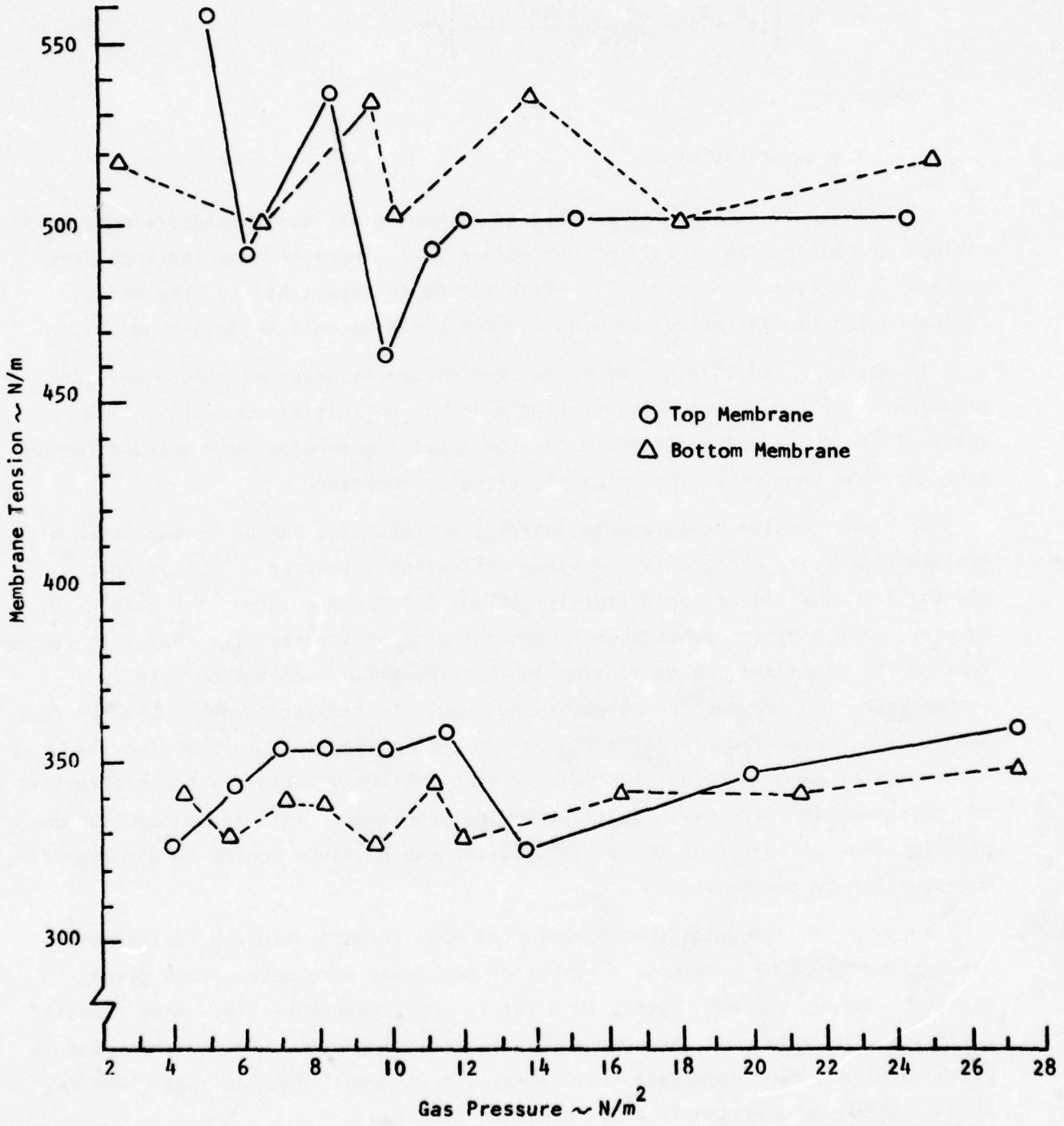

FIGURE 3-14. TYPICAL MEMBRANE TENSION DATA

In the case of Mylar over an organic rubber substrate, no problem was encountered, and tension was measured with this substrate material in place. Tension in latex and neoprene membranes was also easily measured with any of the substrates installed.

3.3 MEMBRANE MATERIALS AND THICKNESSES

Table I provides a summary of the membrane materials and thicknesses tested during this program. The Perflex E* film was eliminated early in the initial tests because of its low resistance to radial wave formation. These waves are characteristic of compliant disks and have been discussed previously by Hansen and Hunston.[5] However, it was established that the formation of these waves could be delayed to 800 rpm ($Re \simeq 4.6 \times 10^6$) by increasing tension in 2 mil Mylar membranes to 800 N/m. This was found to be independent of substrate material, provided the membrane was unbonded. To place this in perspective, Hansen and Hunston reported a wave-onset Reynolds number of 4.2×10^5 for compliant disks consisting of 20% PVC plastisol. Thus, the use of membranes permits a considerable improvement in the Reynolds number at which radial, surface waves begin to form. Of course in the limit as $T \to \infty$, the membrane would become a rigid surface. Therefore, in summary, membrane tension is an important variable which can be used to control compliant wall properties.

Two thicknesses of Mylar were tested in order to investigate the effects of plate bending stiffness which is proportional to thickness cubed. The limited experimental results, reported in the following section, did not indicate any effect of this variable.

*Trademark of Union Carbide.

TABLE I. MEMBRANE MATERIALS AND THICKNESSES

MATERIAL	THICKNESS(cm)
Perflex E	.0051
Mylar	.0025
Mylar	.0051
Latex	.023
Neoprene	.159
Polyurethane	.239
Polyvinyl Chloride	.0076

4.0 EXPERIMENTAL DATA

Moment coefficient data for 36 compliant disks are presented in a normalized form. This form of data presentation is considered to be the most appropriate because it accounts for tank wall effects, changes in bearing friction, instrumentation idiosyncrasies, and any other effects which might cause errors in absolute values of disk drag. The experimental uncertainty in these ratios is estimated to be ± 7%.* However, uncertainty in differences for a given disk or between comparable weight cases is considered to be within ± 4%.

The order of presentation is on the basis of weight, i.e. data for the lightest weight membranes are presented first with substrate weight increasing for a given membrane.

As discussed previously in Sections 2.0 and 3.0, the data include variations of the following variables:

1. Substrate material and thickness;
2. Membrane material, thickness and tension; also whether bonded or unbonded to the substrate.

These variables are identified for each case on Figures 4-1 thru 4-18.

4.1 MOMENT COEFFICIENT DATA

Data for 1 mil Mylar membranes over air substrates are shown in Figure 4-1. Two values of membrane tension were tested with an air gap of 0.132 cm separating the membrane from a styrofoam substrate. This configuration was designed to test the hypothesis of Bushnell et al.[1], viz. membranes over thin air gaps will tend to respond to high frequencies and may be more effective in reducing drag. However, for the two values of membrane tension tested, this arrangement does not appear to be very promising. In fact, the measured drag was lower for the 1 cm air spacing, Figure 4-1. Although the membrane tension is slightly higher for this configuration, the small air gap data do not indicate any significant effect of tension. In all three cases, disk drag was higher than the hard, reference disk.

*The data taken early during the program with nylon drive shaft bearings are high by as much as 10% and represent exceptions to the above uncertainty limits. However, these cases are appropriately noted in the following data discussions.

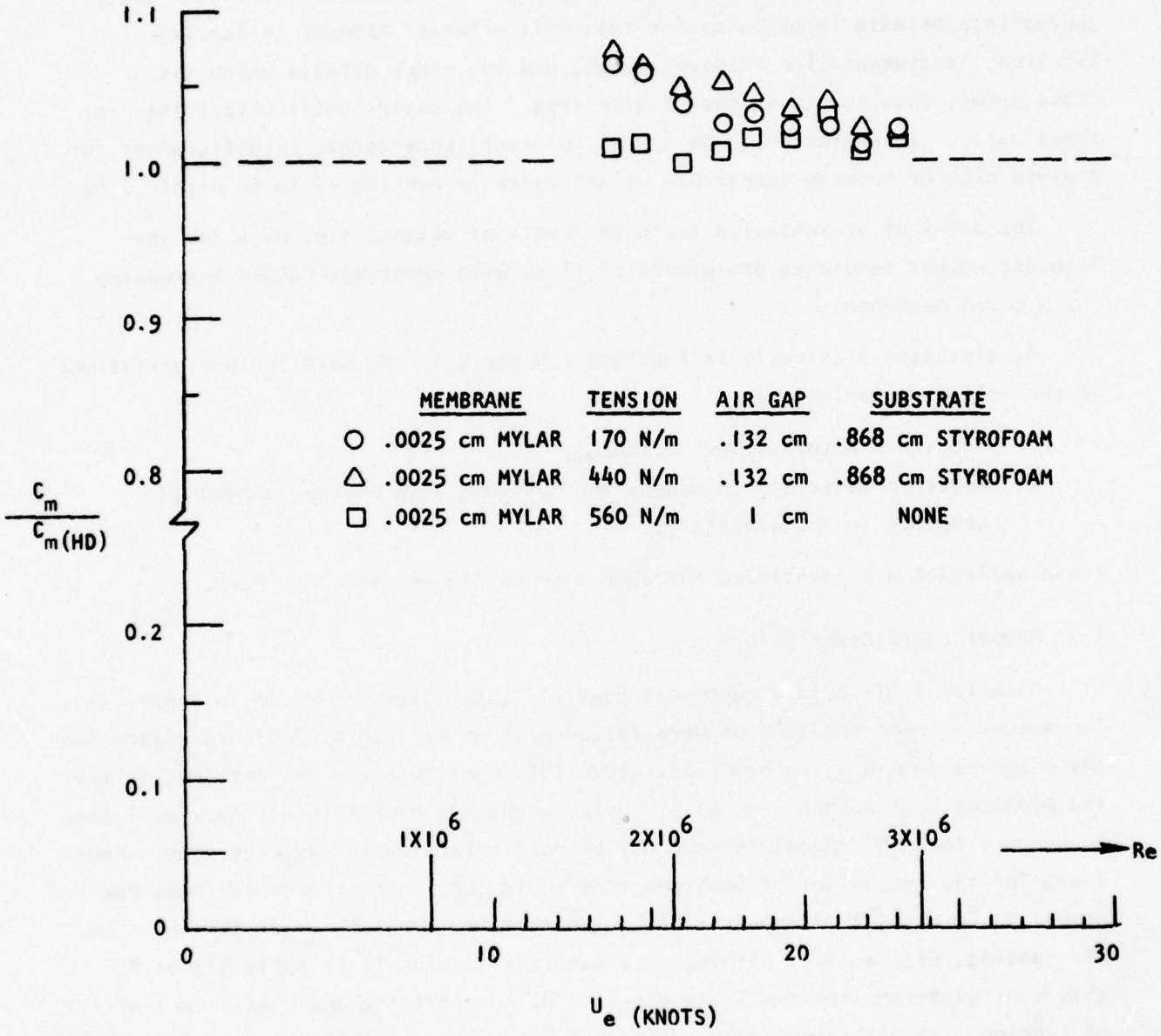

FIGURE 4-1. NORMALIZED MOMENT COEFFICIENT DATA

Figure 4-2 presents drag results for disks with 1 mil Mylar over two thicknesses of polyurethane foam. Membrane tension was held constant at 150 N/m, but was tested both bonded and unbonded to 1/3 cm PU foam with a 2/3 cm styrofoam spacer to fill the disk cavity. There are no detectable differences in drag of the bonded and unbonded cases. With regard to substrate thickness effects, the 1 cm PU foam gave slightly less drag (4 to 2%). In fact, it reproduced the hard disk data quite well. This trend, drag decreasing with increasing substrate thickness, is opposite to what might be expected, since zero thickness PU foam would correspond to the hard disk. However, the small differences in the data lie within the experimental uncertainty, and thus no definitive conclusions can be made.

Data for 1 mil Mylar over 1/3 cm organic rubber are shown in Figure 4-3. The membrane tension was again 150 N/m and was tested bonded and unbonded. The drag level is very similar to the data obtained with 1/3 cm PU foam; only in this case, the bonded case exhibits slightly lower drag. Presumably, this is due to lower response amplitudes in the bonded case.

The same membrane material and tension was tested over 1 cm organic rubber. For this configuration, the bonded and unbonded cases agree within 1%, Figure 4-4. The level of drag is very similar to the data obtained for the 1/3 cm organic rubber. Thus, it is concluded that the drag of 1 mil Mylar-organic rubber disks is insensitive to small changes in substrate thickness.

Figure 4-5 shows the effects of varying tension in 1 mil Mylar bonded to 1 cm organic rubber. Membrane tensions of 0.0, 125 and 190 N/m were tested. There appears to be a slight reduction in drag as tension is varied from zero to 125 N/m. However, there are negligible differences between the 125 and 190 N/m cases, and in all three cases the drag was equal to or greater than the reference values.

Data for the last disk with 1 mil Mylar membranes is presented in Figure 4-6. The membrane was bonded to 20% PVC plastisol with a tension of 160 N/m. The same data is normalized with both styrofoam and plexiglas hard disks in order to illustrate the effects of vibration. The data, normalized with styrofoam, hard disk drag, is generally higher than was measured for lighter weight substrates. When the data is normalized with Plexiglas hard disk drag, the

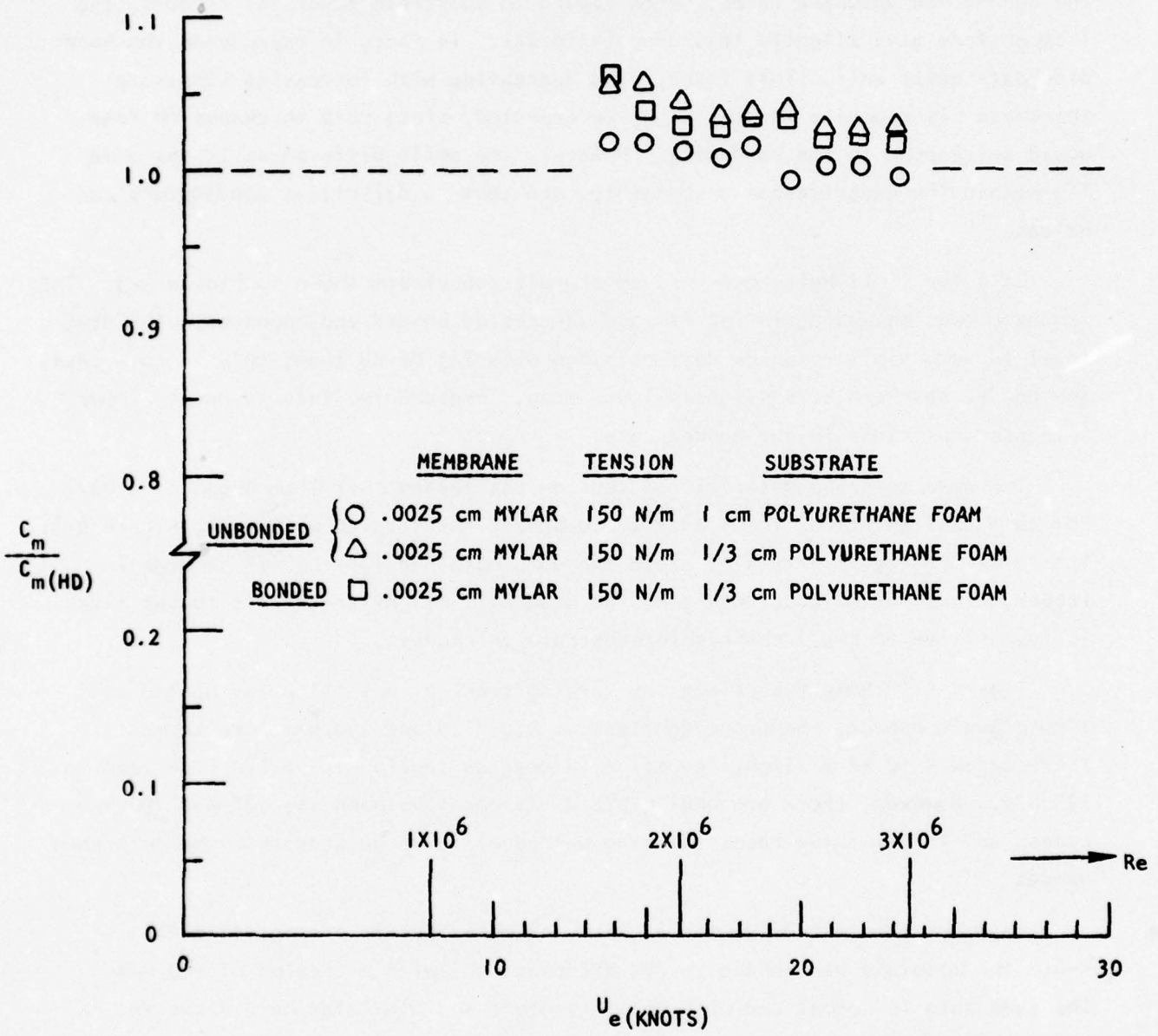

FIGURE 4-2. NORMALIZED MOMENT COEFFICIENT DATA

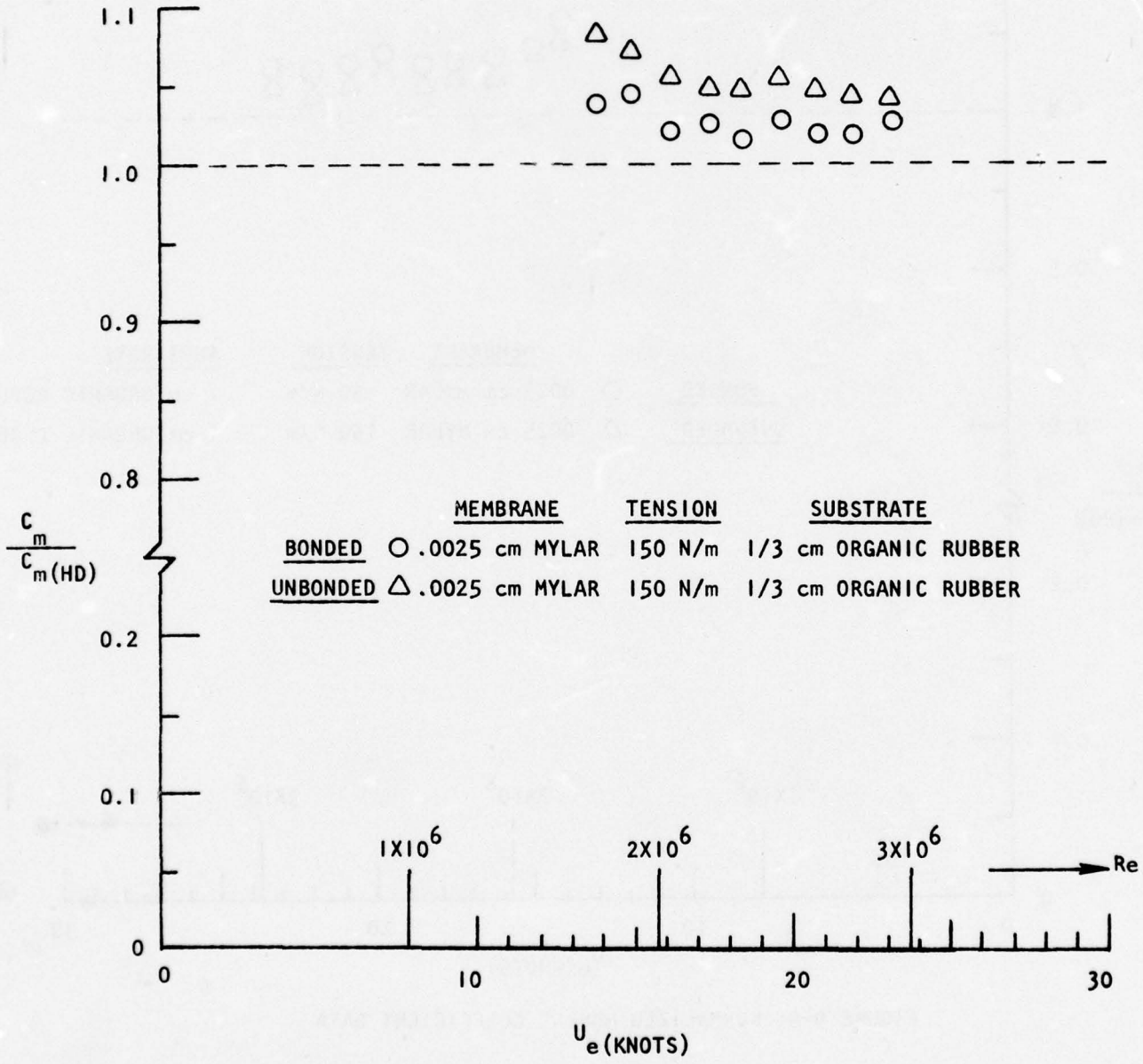

FIGURE 4-3. NORMALIZED MOMENT COEFFICIENT DATA

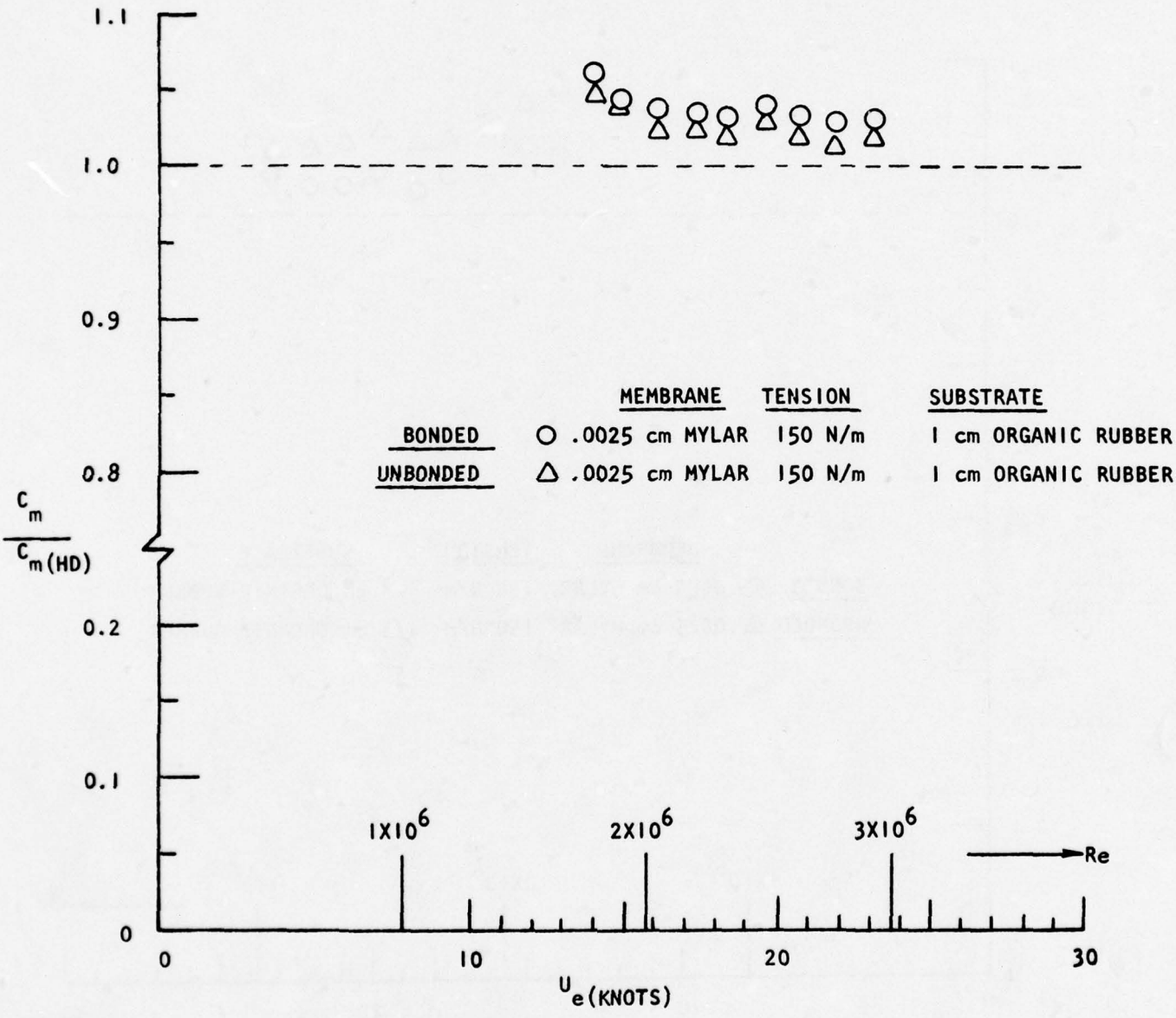

FIGURE 4-4. NORMALIZED MOMENT COEFFICIENT DATA

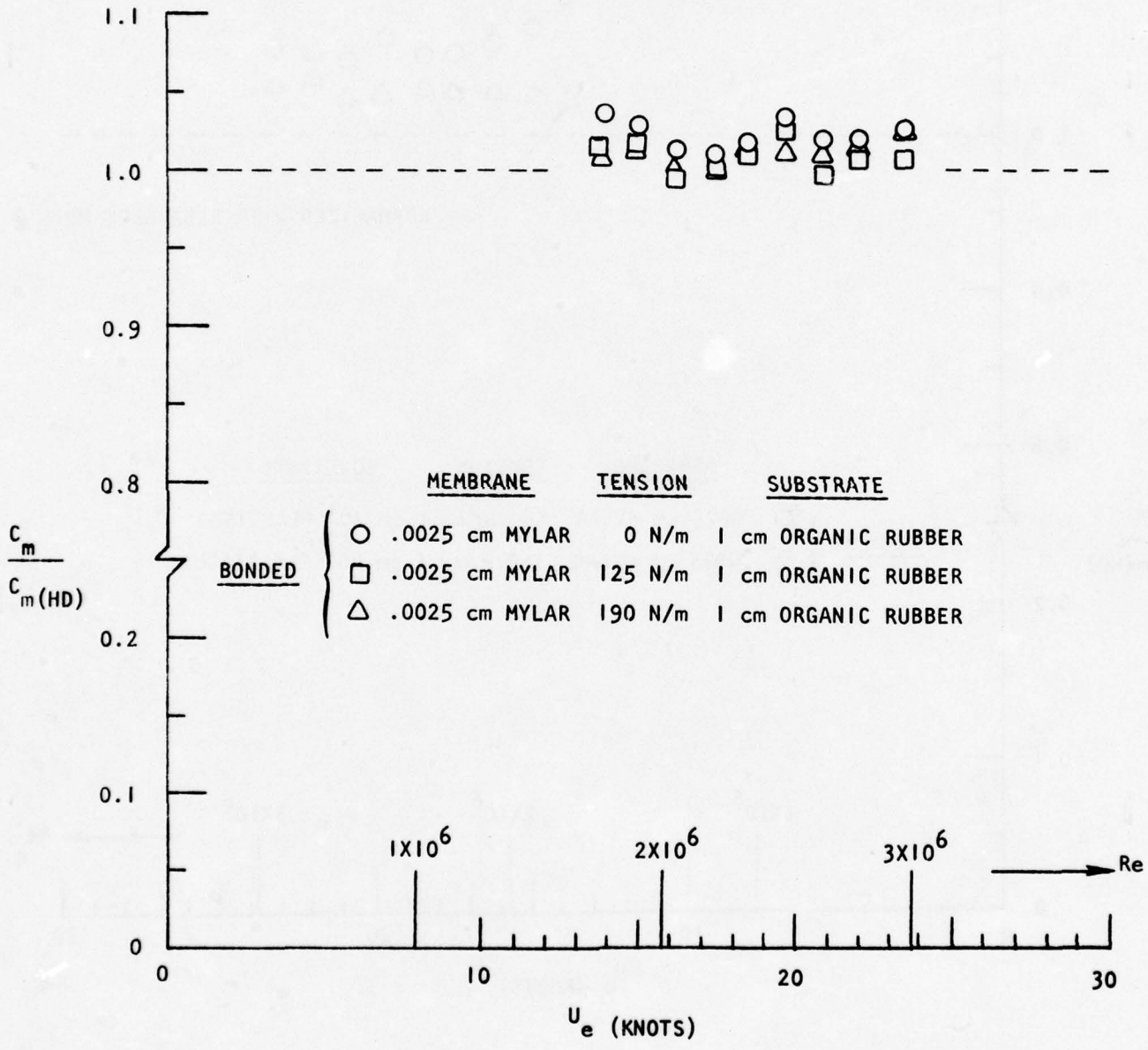

FIGURE 4-5. NORMALIZED MOMENT COEFFICIENT DATA

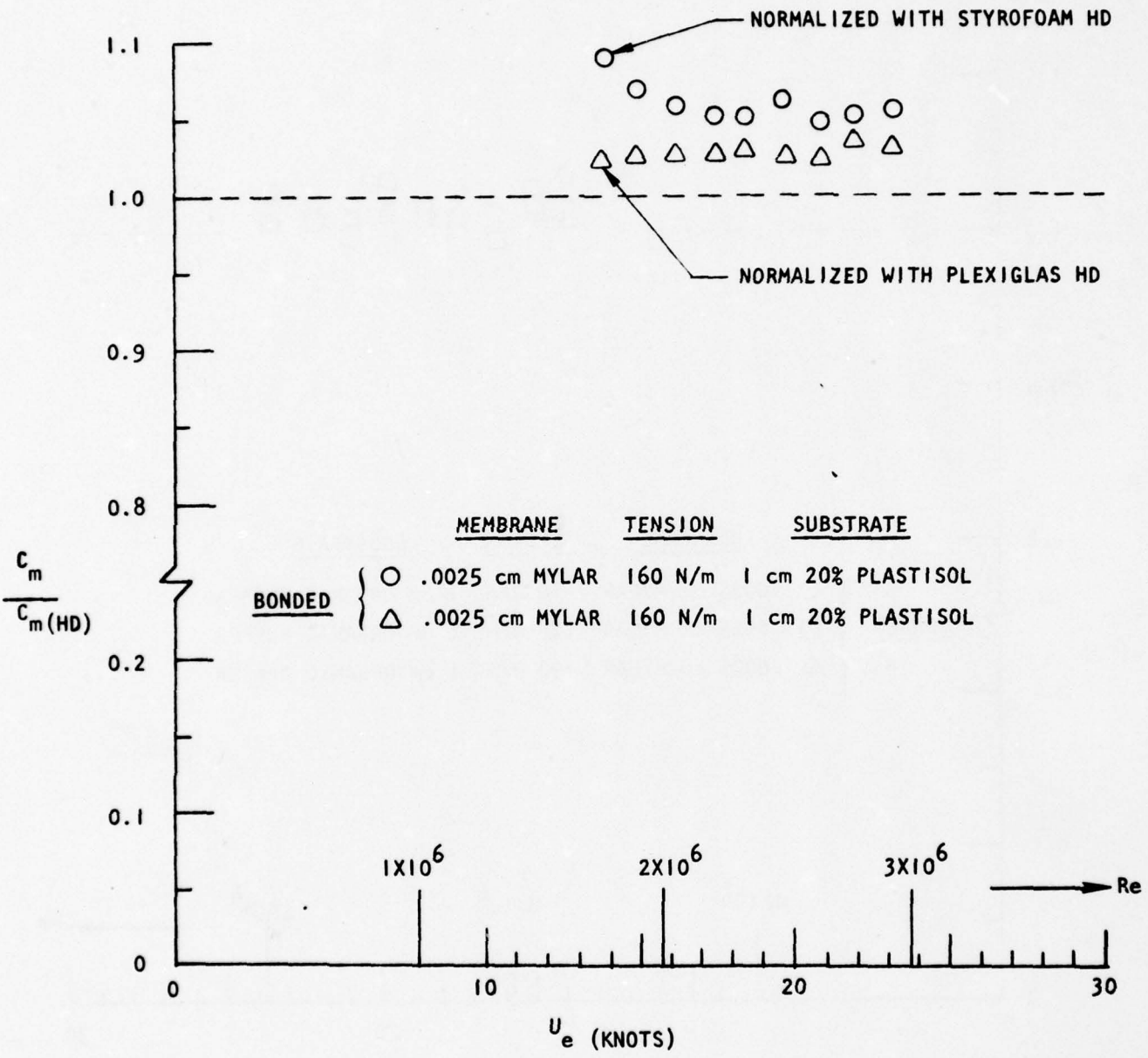

FIGURE 4-6. NORMALIZED MOMENT COEFFICIENT DATA .

moment coefficient ratio drops much closer to one. Since the discussion in Section 2.1 established that the Plexiglas substrates caused significant disk vibration, this form of data presentation indicates the plastisol disks also have significant vibration.

In fact, 20% PVC plastisol is very difficult to place in the disk cavity so that the mass is uniformly distributed. Also, this material deforms under centrifugal loads which can cause further mass imbalance. The resulting transverse vibrations of the disk contribute additional drag.

Finally, it may be noted that the drag (normalized with styrofoam hard disk) appears to be higher at the lowest rpm (low Re) and decreases with increasing rpm.* This indicates that vibration amplitude decreases, rather than increases, with increasing rpm which, in turn, suggests an additional phenomena is involved. It is hypothesized that the drive shaft-disk-water tank system has a natural frequency near 5 Hz. This corresponds to 300 rpm, the beginning rotational speeds for these tests. Calculations, substantiating this hypothesis, are included in later discussions of Figures 4-9 and 4-10.

The next four figures present data for disks with 2 mil Mylar membranes. The effects of varying tension in unbonded membranes over 1 cm polyurethane foam are shown in Figure 4-7. Moments for these cases are 11 to 22% higher than the hard disk, reference values. Observations of these disks with a strobe light did not reveal any standing waves for the given Reynolds number range. However, since these data were taken early in the program, the higher drag is partly attributable to the drive train rather than the disk, See Section 1.2. This conclusion is substantiated by data shown in Figure 4-7 for a bonded membrane. This data was taken after new bearings were installed and agrees closely with the reference values.

Two mil Mylar membranes were also tested over 1 cm organic rubber with a tension of 535 N/m. These data reproduce the reference values within 1%, Figure 4-8.

The differences in drag due to differences in bearing friction are indicated by the data of Figure 4-9. In these cases, 2 mil Mylar was tested unbonded to 1 cm 20% plastisol. Two values of tension (T = 346 and 510 N/m) were tested with

*This phenomena is particularly noticeable in Figures 4-9 and 4-10.

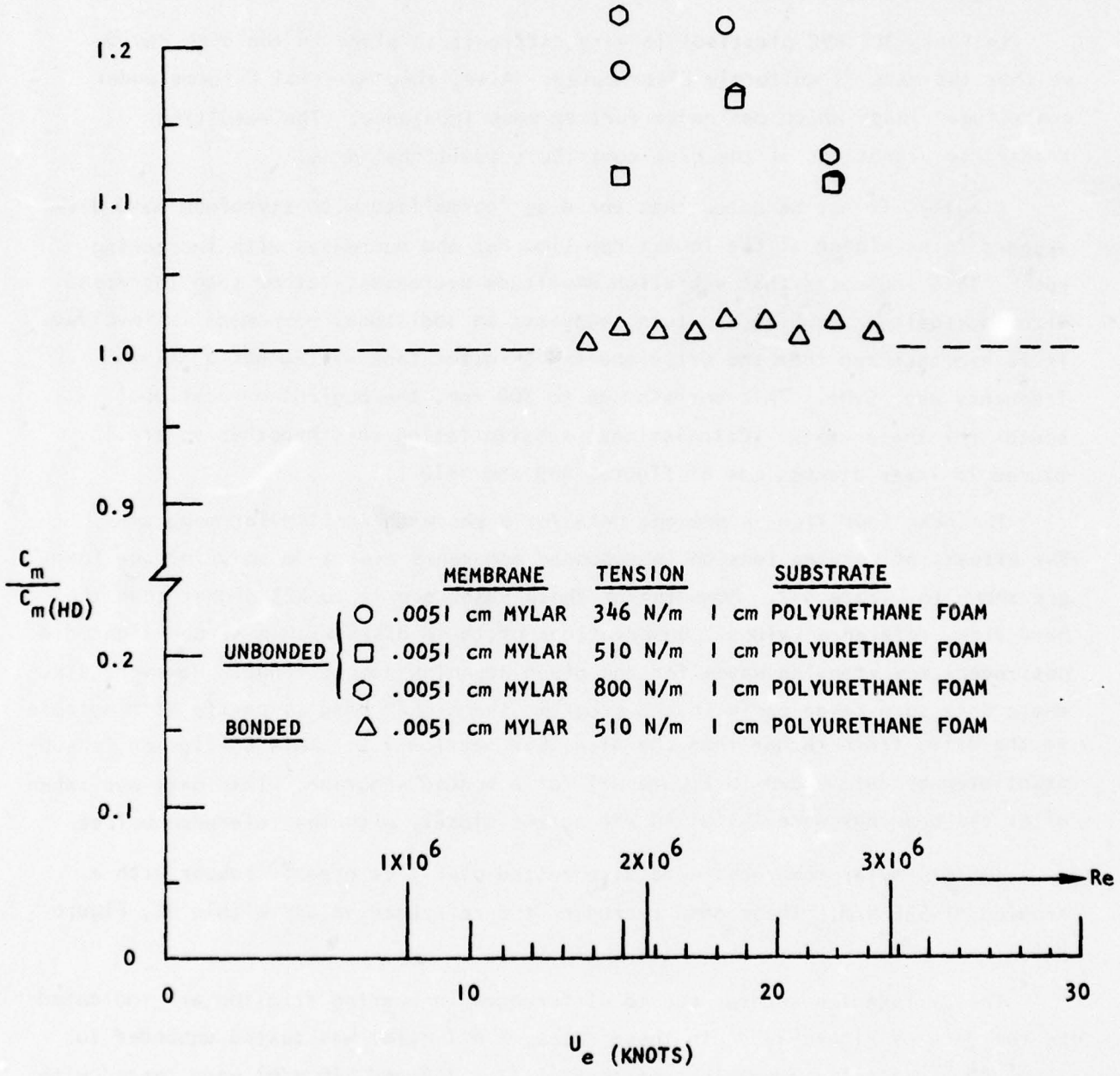

FIGURE 4-7. NORMALIZED MOMENT COEFFICIENT DATA

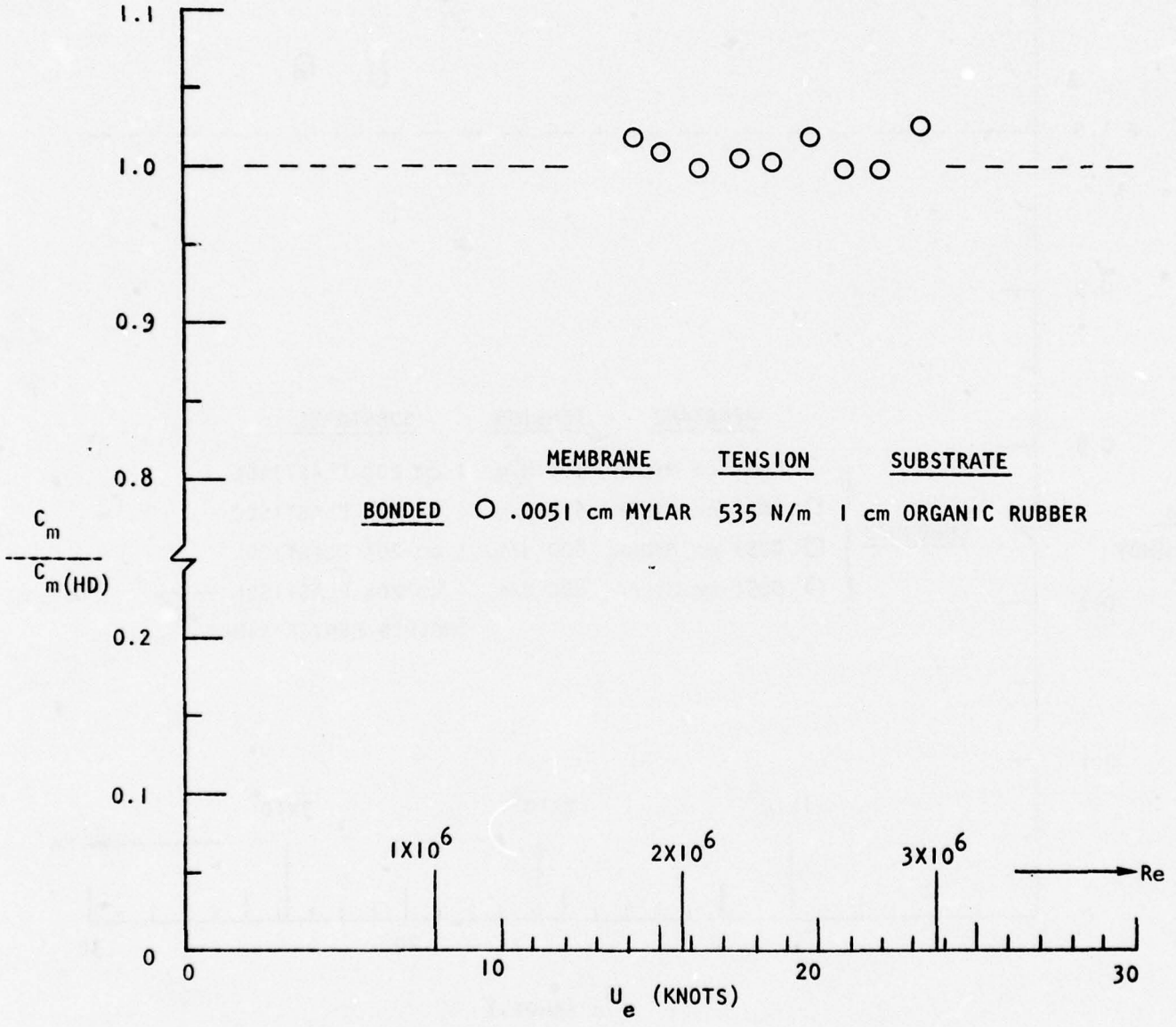

FIGURE 4-8. NORMALIZED MOMENT COEFFICIENT DATA

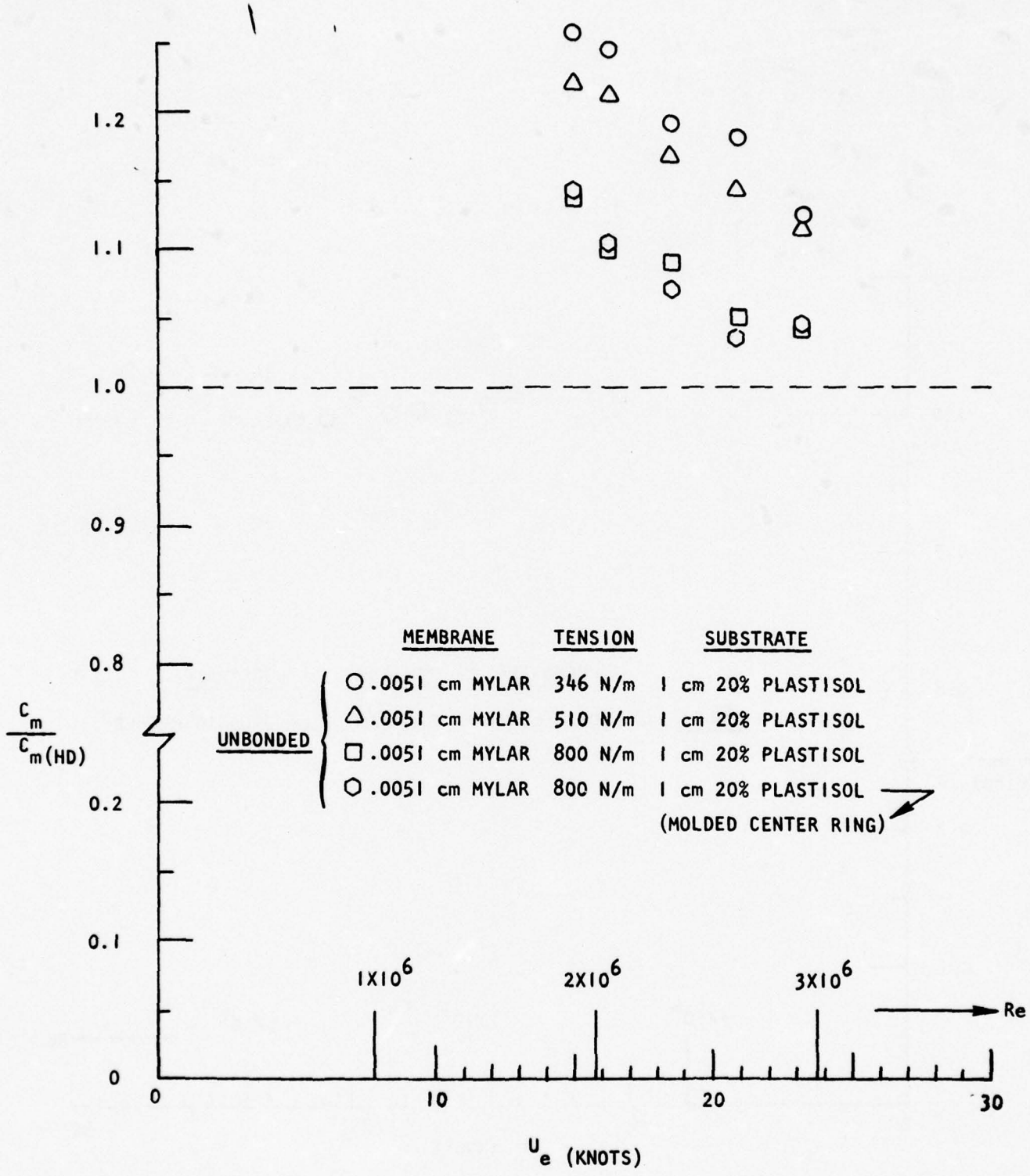

FIGURE 4-9. NORMALIZED MOMENT COEFFICIENT DATA

with the old bearings, and one value (T = 800 N/m) was tested twice with the new bearings. Assuming negligible tension effects, the old bearings caused the measured drag to be approximately 10% high.

The second test with T = 800 N/m was conducted with a set of 20% plastisol substrates having small aluminum center rings molded into them. This was observed to be effective in preventing the substrate from pulling away from the center hub during spinning. However, this had no significant effect on disk drag, Figure 4-9.

The effects of varying resin content in PVC plastisol substrates is shown in Figure 4-10. The lowest drag was measured for the case of 20% plastisol. However, since the highest drag was measured for the case of 25% plastisol and the total spread in the data is approximately 6%, no definite conclusions can be made concerning the superiority of one substrate.

Irrespective of differences in bearing friction and data scatter, Figures 4-9 and 4-10 show a rather rapid decline in drag of plastisol disks with increasing rpm. This is suggestive of a corresponding decay in amplitude of vibration. If this is true, the combined system of drive shaft-disk-water tank must have a natural frequency near 5 Hz. This would explain the decay in amplitude as the rotational speeds moves away from a resonant condition. This hypothesis is supported by the following calculations.

The fundamental natural frequency of a uniform cantilever (in vacuo) is given by

$$\omega_1 = (1.875)^2 \, (EI/m\ell^4)^{1/2}, \qquad (4\text{-}1)$$

where

E = Young's modulus

I = Moment of inertia of cross section

m = Mass per unit length

ℓ = Length of cantilever.

The corresponding frequency for the bare drive shaft used in these tests is 52.6 Hz. If a weight is added to the free end of a cantilever, the natural frequency is reduced and may be calculated from (McLachlan[16])

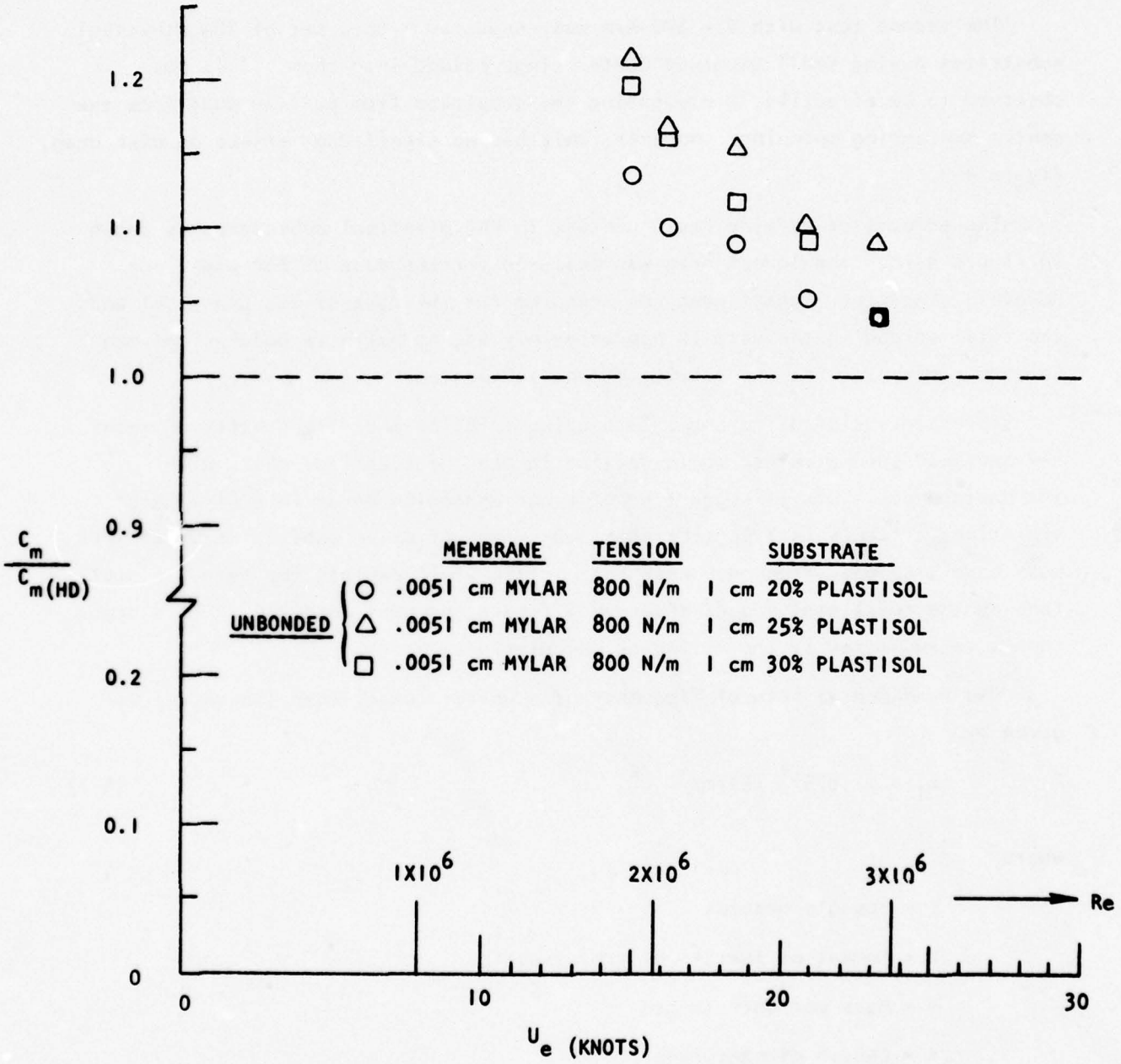

FIGURE 4-10. NORMALIZED MOMENT COEFFICIENT DATA

$$\omega_1 \approx \left(\frac{3EI}{W\ell^3}\right)^{1/2} \left(1 - \frac{33m_c}{280W}\right), \qquad (4\text{-}2)$$

where

W = Mass at end of cantilever

m_c = Total mass of cantilever.

Substituting the appropriate values for the drive shaft and the weight of a plastisol disk, a natural frequency of 13.7 Hz is obtained. Finally, when it is realized that the water also adds an induced mass to the system, a natural frequency of 5 Hz (or less) for the complete system is quite plausible.*

The next weight membrane is 3 mil vinyl. From common experience, it is known that vinyl is quite soft and pliable. In fact, we were unable to obtain a tension measurement on membranes made of this material because the applied gas pressures caused the vinyl to creep and change deflection while pressure was held constant. This characteristic of thin vinyl prevents application of a known tension. Thus, during the fabrication of these disks a low, but sufficient, tension was applied to remove wrinkles in the surface. The resulting membranes appeared to be smooth and free of wrinkles immediately prior to insertion in the water tank.

The first test of vinyl was conducted with the membrane unbonded to 1 cm polyurethane foam. Standing waves were observed at the beginning rpm and resulted in drag being approximately 10% higher than the reference values, Figure 4-11. A photograph of typical standing waves is reproduced in Figure 4-12.

Subsequently, vinyl membranes were bonded to 1 cm polyurethane foam and organic rubber. This did indeed delay the formation of standing waves. However, with the exception of one data point, no significant drag reduction was measured, Figure 4-11. Although a drag reduction of 4% is indicated at the initial rpm for the vinyl/PU foam case, this is within the experimental uncertainty (±7%) and is not considered to be a clear case of drag reduction. Figure 4-13 is an interesting photograph of the severe deformation that occurred when the disk, with vinyl bonded to polyurethane foam, was tested at higher rpm's.

The thin mylar and vinyl membranes were tested based on the success Walters[7], Mattout[8], and Weinstein and Fischer[9] reported using these materials

*In the cases of lighter weight substrates, the imbalance forces are apparently so small that transverse vibrations are not excited.

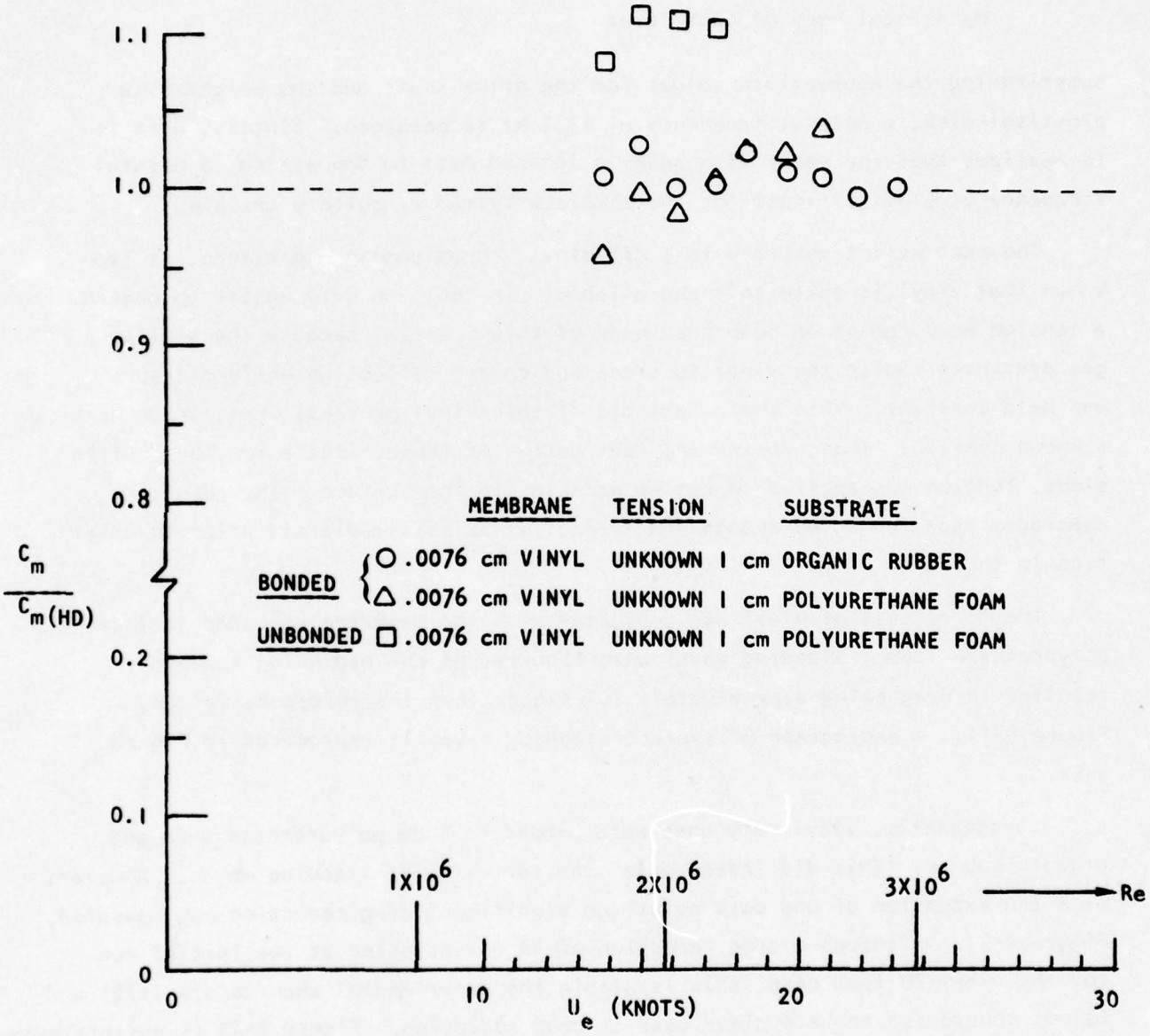

FIGURE 4-11. NORMALIZED MOMENT COEFFICIENT DATA

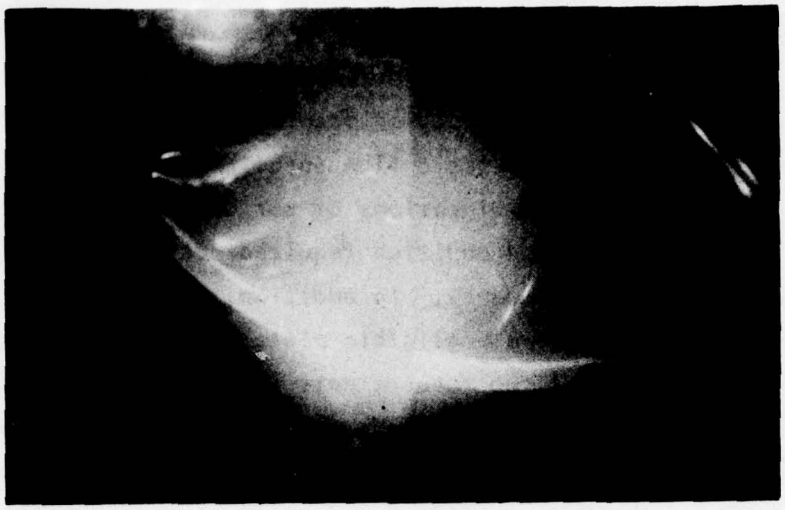

FIGURE 4-12. STROBELIGHT PHOTOGRAPH OF RADIAL WAVES WHICH OCCUR AT HIGHER RPM'S

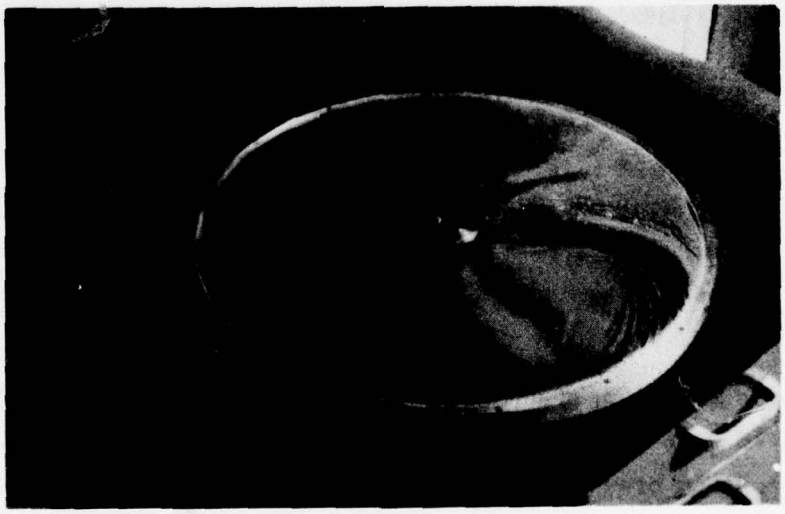

FIGURE 4-13. SEVERE DEFORMATION OF 3 MIL VINYL BONDED TO POLYURETHANE FOAM SUBSTRATE

on flat plates. Unfortunately, these thin, light weight membranes were singularly unsuccessful in reducing hydrodynamic drag of rotating disks. The only other existing tool for guiding the selection of membranes was the frequency correlation of Ash.[10] This correlation of reported drag reductions on flat plates with membranes indicates maximum reduction occurs when the natural frequency of the membrane is 1/2 of a characteristic flow turbulence frequency. In the case of an annular membrane, with the dimensions of our disk and subject to the flow conditions of these tests, Ash's condition required heavier membrane materials in order to reduce the natural frequency. In addition, it was also desirable to select materials which would have negligible plate bending stiffness. In order to approximately satisfy these two requirements, membranes were fabricated using five sheets of 0.023 cm latex bonded together. The resulting frequency ratios are discussed in Section 4.2. The corresponding moment coefficients are shown in Figure 4-14. The data indicate a drag reduction of approximately 5% occurred at the beginning Reynolds number. This result must be viewed with caution since it is within the experimental uncertainty (± 7%). The rapid rise in drag with increasing rpm is associated with the initiation of standing waves.

Neoprene rubber was next selected as a candidate for a heavier membrane material. A military grade of neoprene was used because of its smoother surface finish. Disk drag for the case of 0.16 cm neoprene membranes over 1 cm polyurethane foam is shown in Figure 4-15. A drag increase of five to three per cent was measured.

Data for a compound membrane is also included in Figure 4-15. This membrane was designed to see if a light weight membrane might respond to the turbulence and pass its energy on to a heavier, foundational membrane. Unfortunately, standing waves occurred in the single sheet of latex and caused approximately 10% higher drag. The use of compound membranes is an unexplored possibility and, in the author's opinion, is worthy of further study.

As indicated by the drag data shown in Figure 4-16, very severe standing waves occurred in 0.16 cm neoprene membranes when they were bonded, with near zero tension, to 1 cm organic rubber substrates. This is a good example of the effect of membrane tension, i.e. nonzero tension is essential whether the membrane is bonded or unbonded to a compliant substrate.

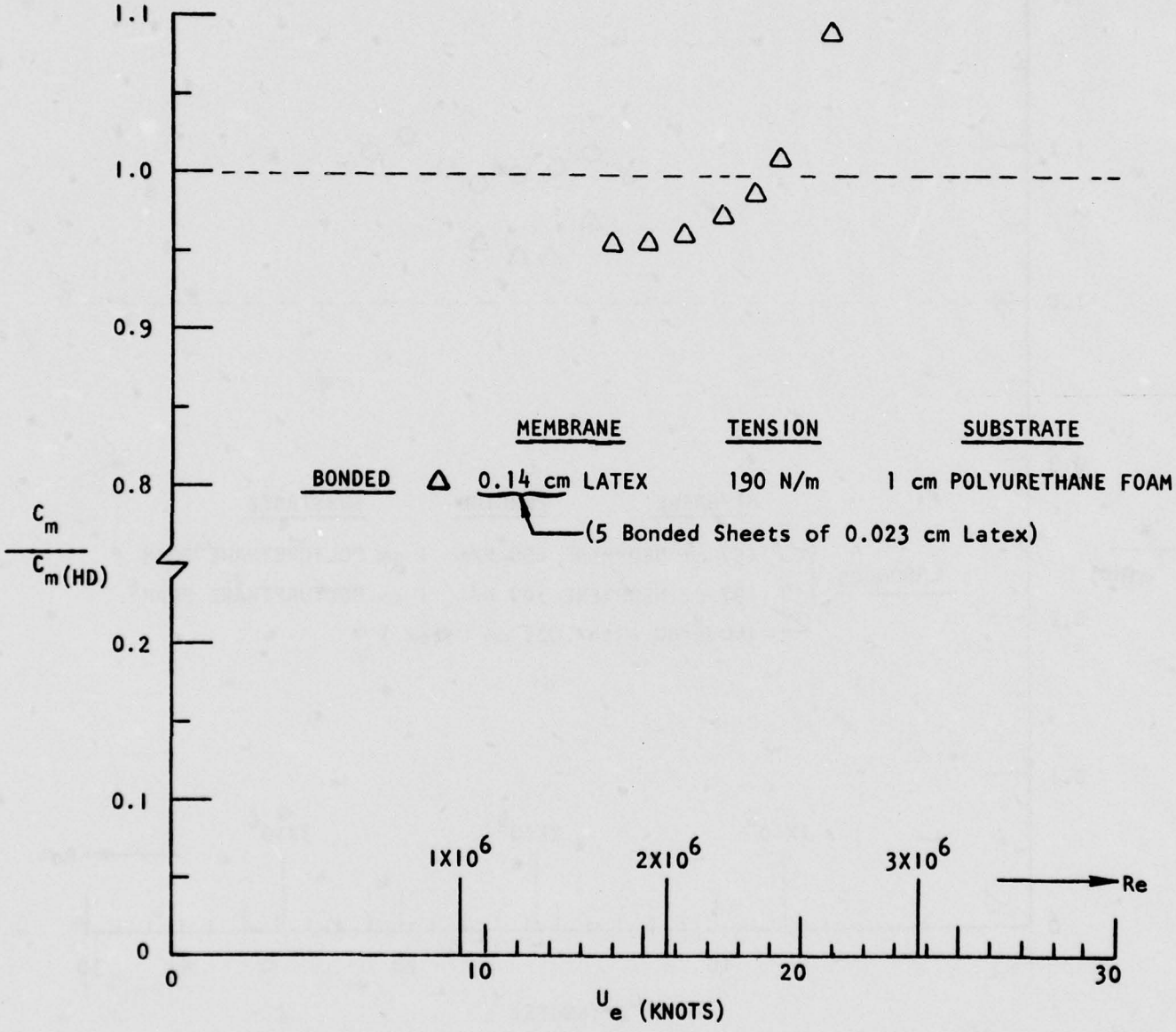

FIGURE 4-14. NORMALIZED MOMENT COEFFICIENT DATA

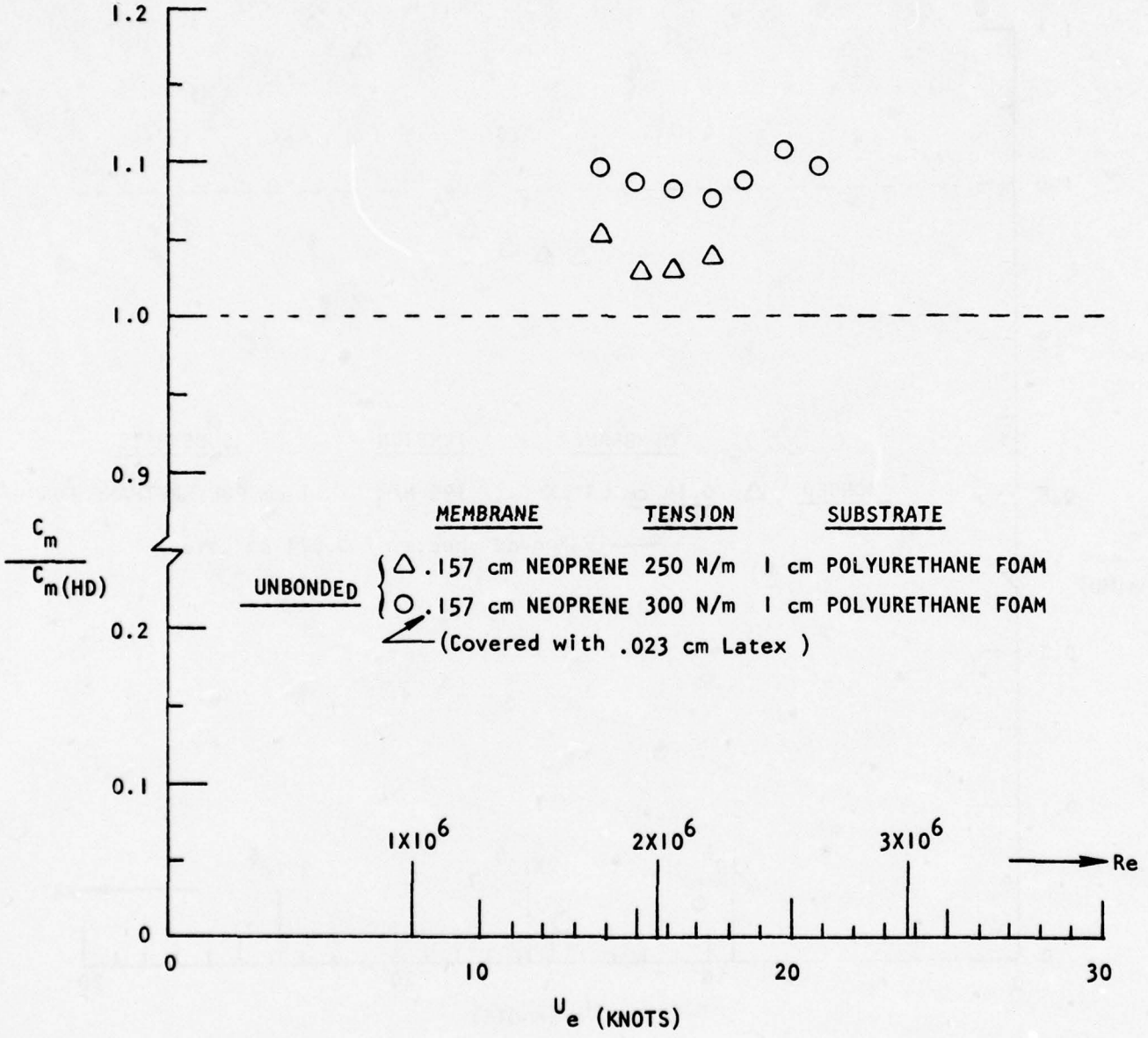

FIGURE 4-15. NORMALIZED MOMENT COEFFICIENT DATA

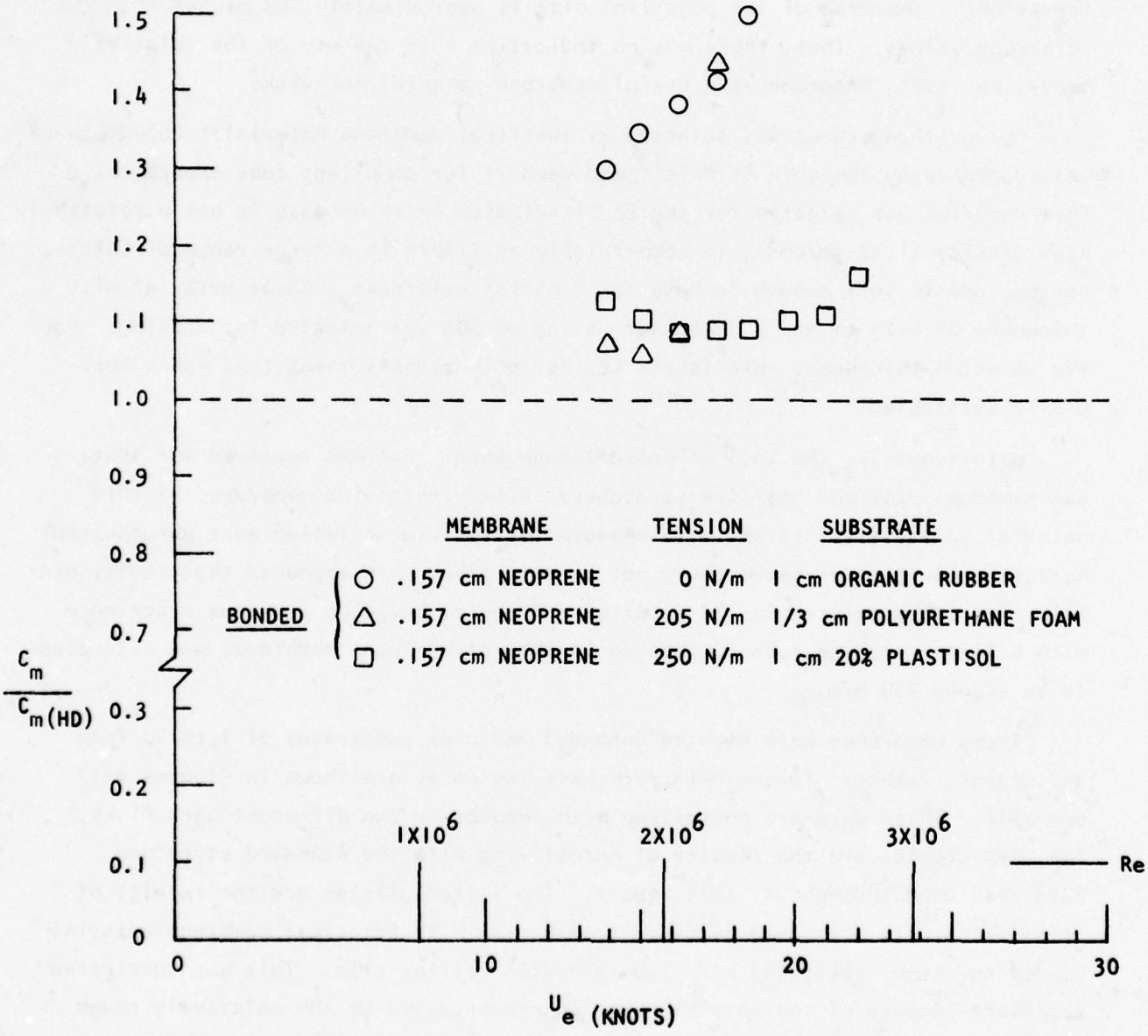

FIGURE 4-16. NORMALIZED MOMENT COEFFICIENT DATA

The same neoprene material was tested with it bonded to 1/3 cm polyurethane foam and 1 cm 20% plastisol. In the case of the PU foam substrate, the membrane tension was 205 N/m and standing waves formed very suddenly near 2.2 million Reynolds number which caused more than a 30% jump in drag, Figure 4-16. Comparison of data for neoprene membranes unbonded to 1 cm PU foam and bonded to 1/3 cm PU foam indicates no significant difference in drag level (prior to radial wave formation). The drag of the plastisol disk is approximately 10% higher than the reference values. Thus, there was no indication that the use of the relatively heavy, but soft, neoprene is a useful membrane material for disks.

Polyurethane sheet was selected as the final membrane material. Polyurethane was suggested by the work of Pelt[17] who used it for compliant tube experiments. This material was selected for the compliant disk tests because it has a relatively high density (1.22 gm/cm^3), is commercially available in a large range of thicknesses, and is soft enough to have low flexural stiffness. Sheet material with a thickness of 0.24 cm and a durometer rating of 50A was selected for testing. For the selected thickness, this is the softest polyurethane sheet that was commercially available.

Unfortunately, the roll of polyurethane sheet that was received for testing had numerous pits and hairline scratches. After installing membranes of this material on the disk, attempts to measure tension via inflation were unsuccessful because a constant pressure could not be maintained. It appeared that small, pinhole size leaks existed in the material. However, based on previous experience with 0.16 cm neoprene rubber, tension in the polyurethane membranes was estimated to be around 250 N/m.

These membranes were mounted unbonded and over substrates of 1 cm PU foam and organic rubber. Torque data for these two cases are shown in Figures 4-17 and 4-18. These data are normalized with respect to two different hard disks. The open circles are the results of normalizing with the standard styrofoam hard disk used throughout this report. The filled circles are the results of normalizing with drag data obtained from a disk with identical membrane material bonded to rigid substrates made from asbestos ceiling tile. This was considered necessary because of the possible drag increase caused by the relatively rough polyurethane. It is readily seen that the two sets of different hard disk data makes considerable difference in the ratio of moment coefficients. In the case of PU

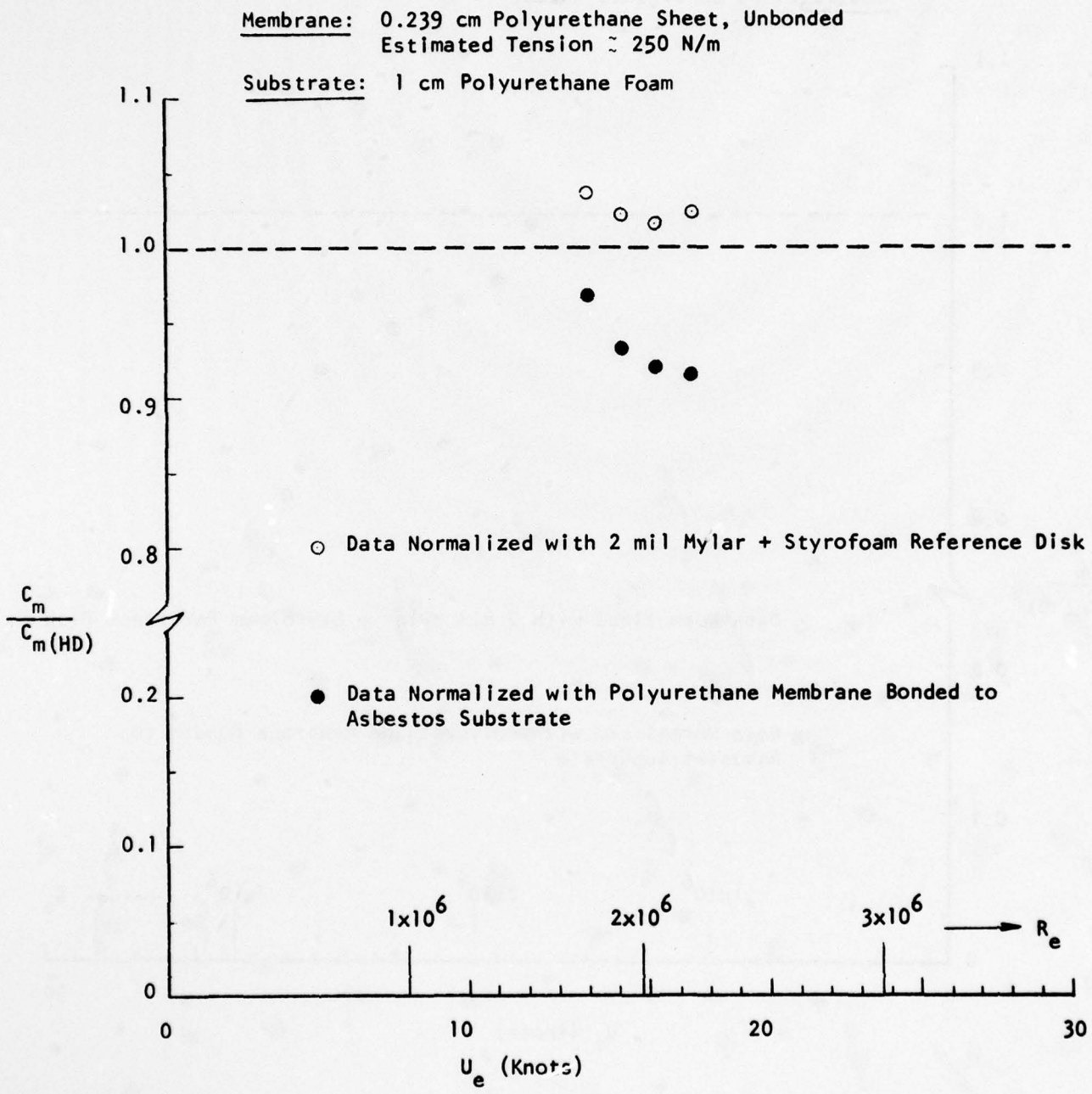

FIGURE 4-17. NORMALIZED MOMENT COEFFICIENT DATA

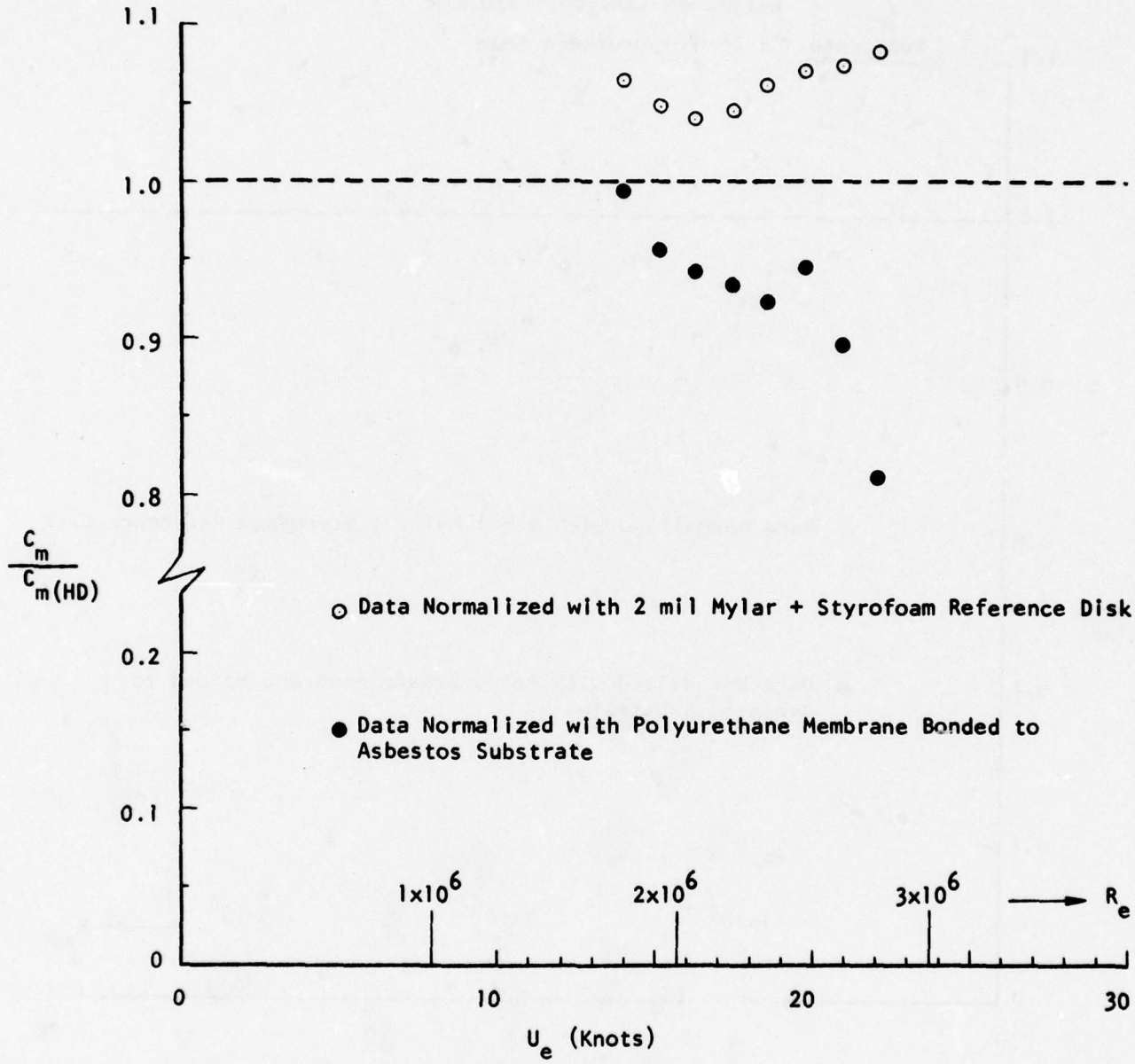

FIGURE 4-18. NORMALIZED MOMENT COEFFICIENT DATA

foam substrates, there is a full 10% difference in drag between the two methods of data presentation. A maximum drag reduction of 8.5% is obtained at the highest Reynolds number by normalizing the PU foam data with the corresponding asbestos hard disk data. The PU foam substrate allowed sudden formation of large, radial waves immediately after the last data point shown in Figure 4-17. Thereafter, the drag increased 50% and was unsteady.

As indicated in Figure 4-18, a drag reduction of 19% is obtained at the highest Reynolds number by normalizing the organic rubber data with the abestos substrate data.* A definite indication of resonance was observed with these heavy membranes. The tank sidewalls were observed to noticeably vibrate at the flow conditions corresponding to the open circle minimums of Figures 4-17 and 4-18. These vibrations could not be felt at lower Reynolds numbers nor at any condition with other disks.

However, it must be emphasized that a disk with drag less than the styrofoam hard disk was not directly measured. Instead, an increase in drag was measured which is presumed to be caused by roughness of the polyurethane membrane. This apparent roughness effect is illustrated in Figure 4-19. Drag of the disk with polyurethane membranes bonded to rigid substrates is 9 to 33% higher than the corresponding drag of the reference disk with mylar bonded to rigid substrates.

In order to obtain a more direct comparison of surface roughness, a Mitutoyo Surftest B (Model 178-904) was used to measure surface roughness. This instrument traverses a stylus ($r = 12.5\ \mu$ with a force < 1.5 gm) over the surface being measured and provides a readout of the rms surface roughness. The 2 mil mylar measured 0.25-0.30 microns; whereas, the polyurethane measured 0.76-2.3 microns. Although this is a significant difference, it is suspected that an even larger difference actually exists because surface irregularities in the much softer polyurethane would tend to be pressed down and smoothed by the stylus.

*It is relevant to here note the organic rubber ($E = 2.45 \times 10^5\ N/m^2$) substrates delayed the formation of standing waves relative to the PU foam ($E = 3.45 \times 10^4\ N/m^2$) substrates.

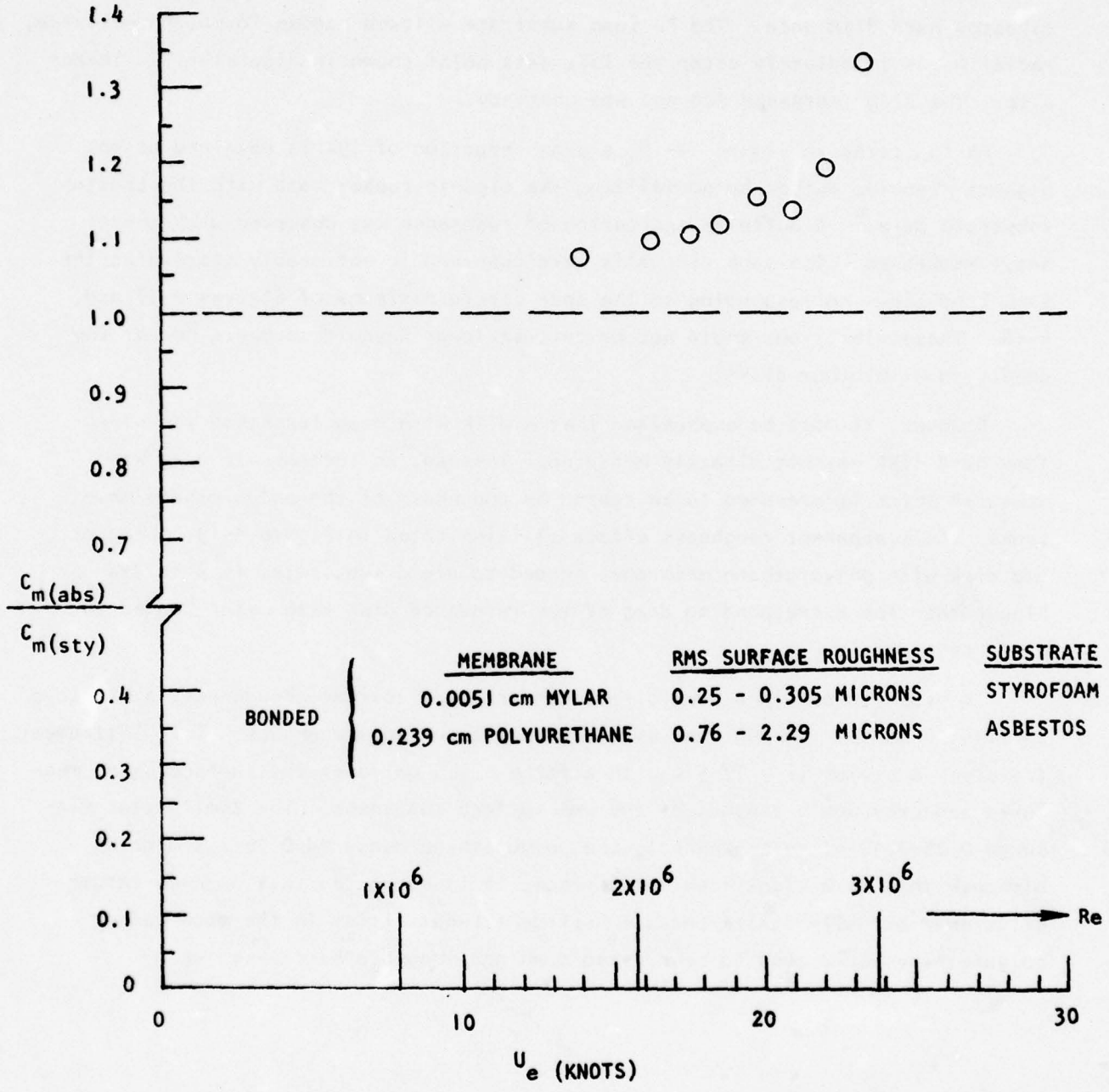

FIGURE 4-19. RATIO OF MOMENT COEFFICIENT FOR ASBESTOS & STYROFOAM HARD DISKS

4.2 ASH'S MEMBRANE FREQUENCY CORRELATION

As mentioned previously, a relatively heavy membrane is required for the 45.7 cm diameter disk in order to evaluate the usefulness of Ash's[10] frequency correlation of previous compliant, flat plate data. This correlation suggests that the ratio of the natural frequency of a membrane should be approximately 1/2 of the peak power frequency of the turbulence. Ash suggested the characterizing frequency of boundary layer turbulence be calculated using

$$F_{peak} = U_\infty / 2\pi\delta \quad . \tag{4-3}$$

This can be adapted to the case of a rotating disk by assuming $U_\infty = \omega r$ and employing an expression developed by Cooper for boundary layer thickness on a rotating disk, viz.

$$\delta = 0.184\ r^{0.75}(\nu/\omega)^{0.125} \quad . \tag{4-4}$$

A representative value for r is 11.4 cm, the distance from the spin axis to the half-radius of the annular membrane. The resulting flow frequencies vary from 138 Hz at 300 rpm to 245 Hz at 500 rpm. The distribution of these frequencies with rpm are shown in Figure 4-20. As an indication of how the frequencies vary across a face of the disk, flow frequencies at the outer radius of the membrane are also included in Figure 4-20.

Ash found that most of the data from previously reported cases of drag reduction fell within the band shown in Figure 4-21. The corresponding data for the disks with polyurethane membranes show a very similar trend. The fundamental frequencies of the annular membranes were calculated by using (e.g. McLachlan[16])

$$F_{vib} = 0.262\ (T \times 10^3/M_m)^{1/2} \tag{4-5}$$

where T = Membrane tension ~ N/m

M_m = Membrane mass per unit area ~ gm/cm^2

Unfortunately, the corresponding data for latex (Figure 4-14) and neoprene (Figure 4-15) membranes over 1 cm polyurethane foam do not show a similar trend, see Figure 4-22.

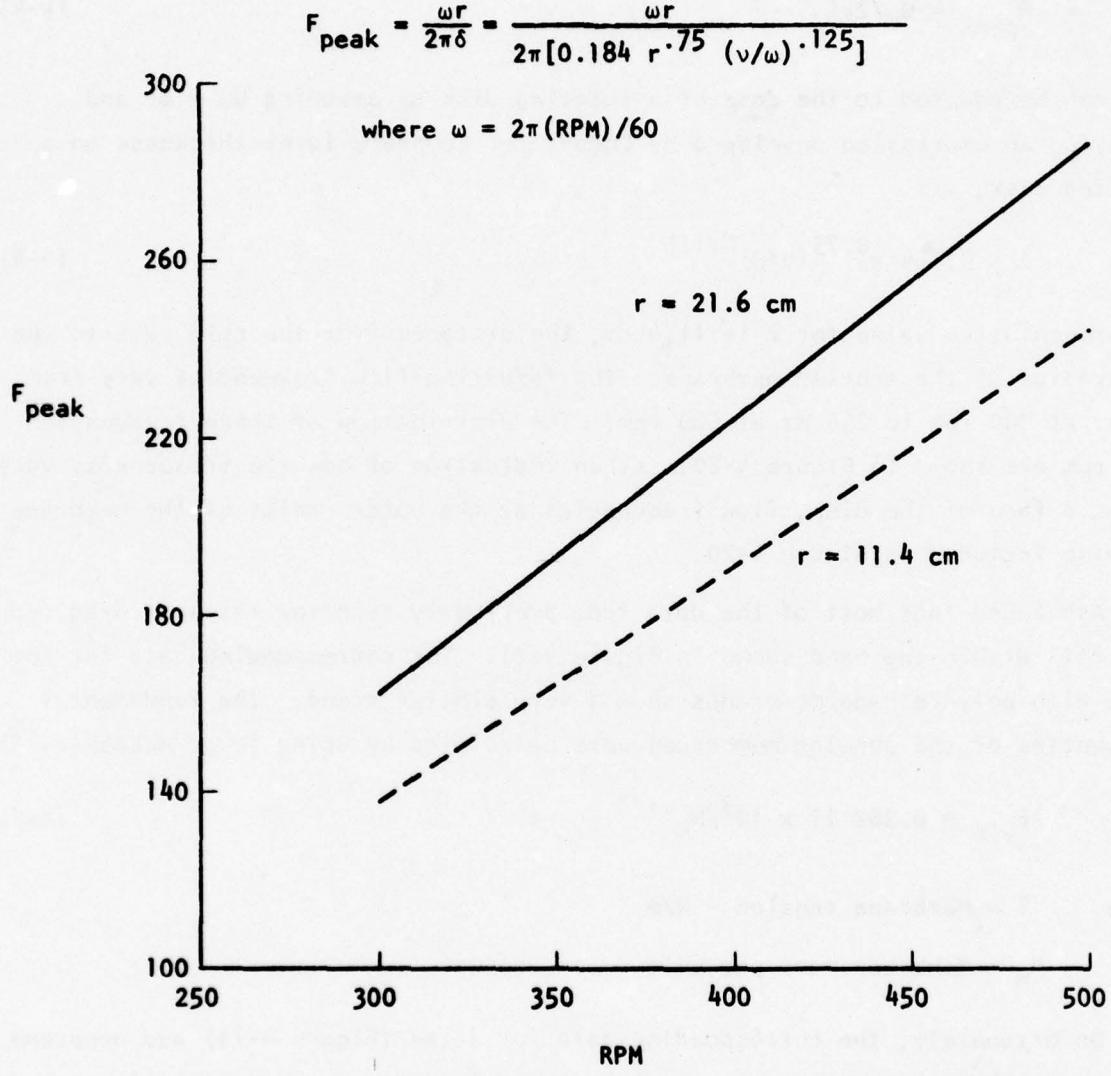

FIGURE 4-20 CHARACTERISTIC FREQUENCIES OF TURBULENT BOUNDARY LAYER ON ROTATING DISK

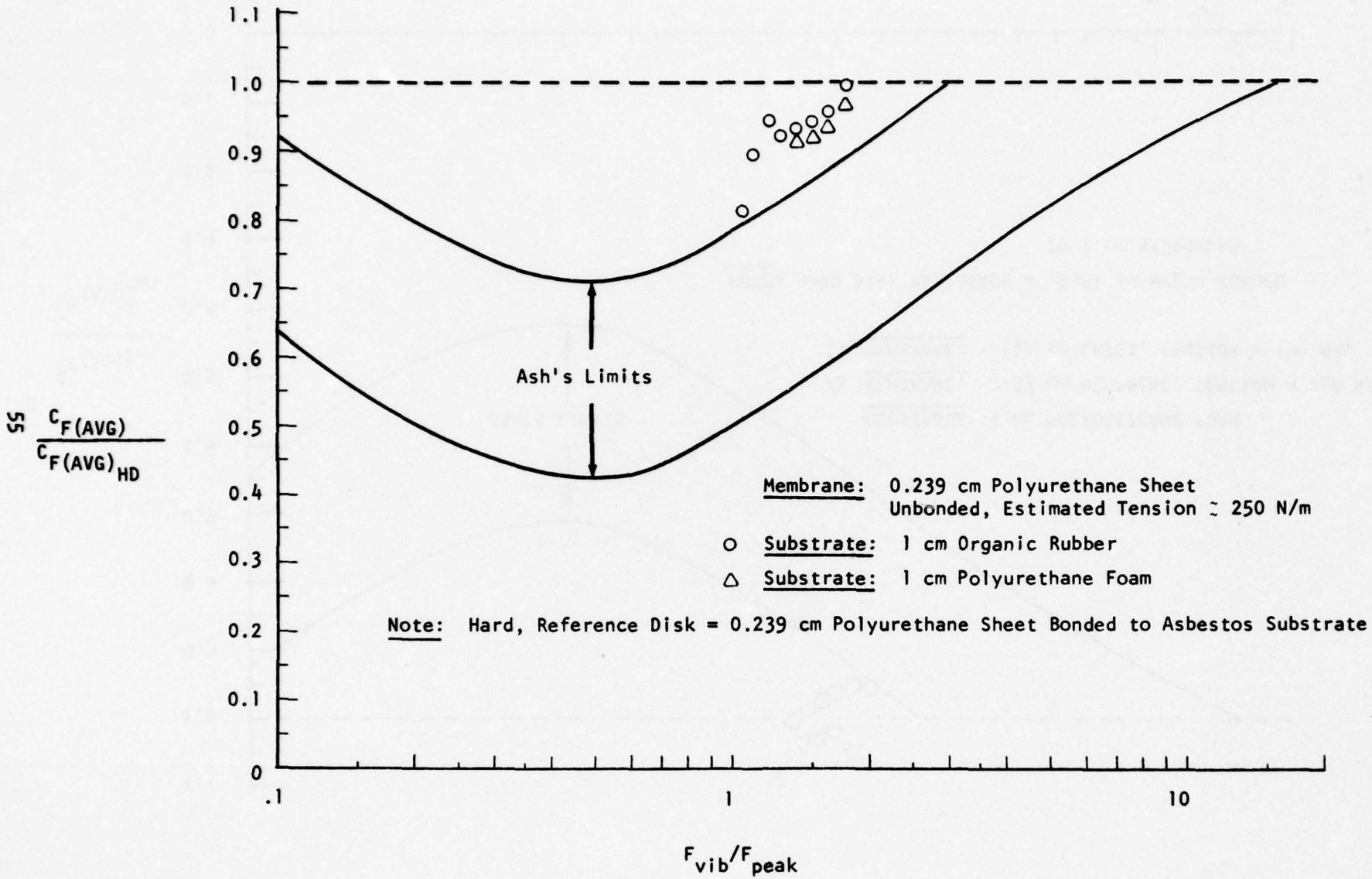

FIGURE 4-21. FREQUENCY DATA FOR DISKS WITH HEAVY MEMBRANES

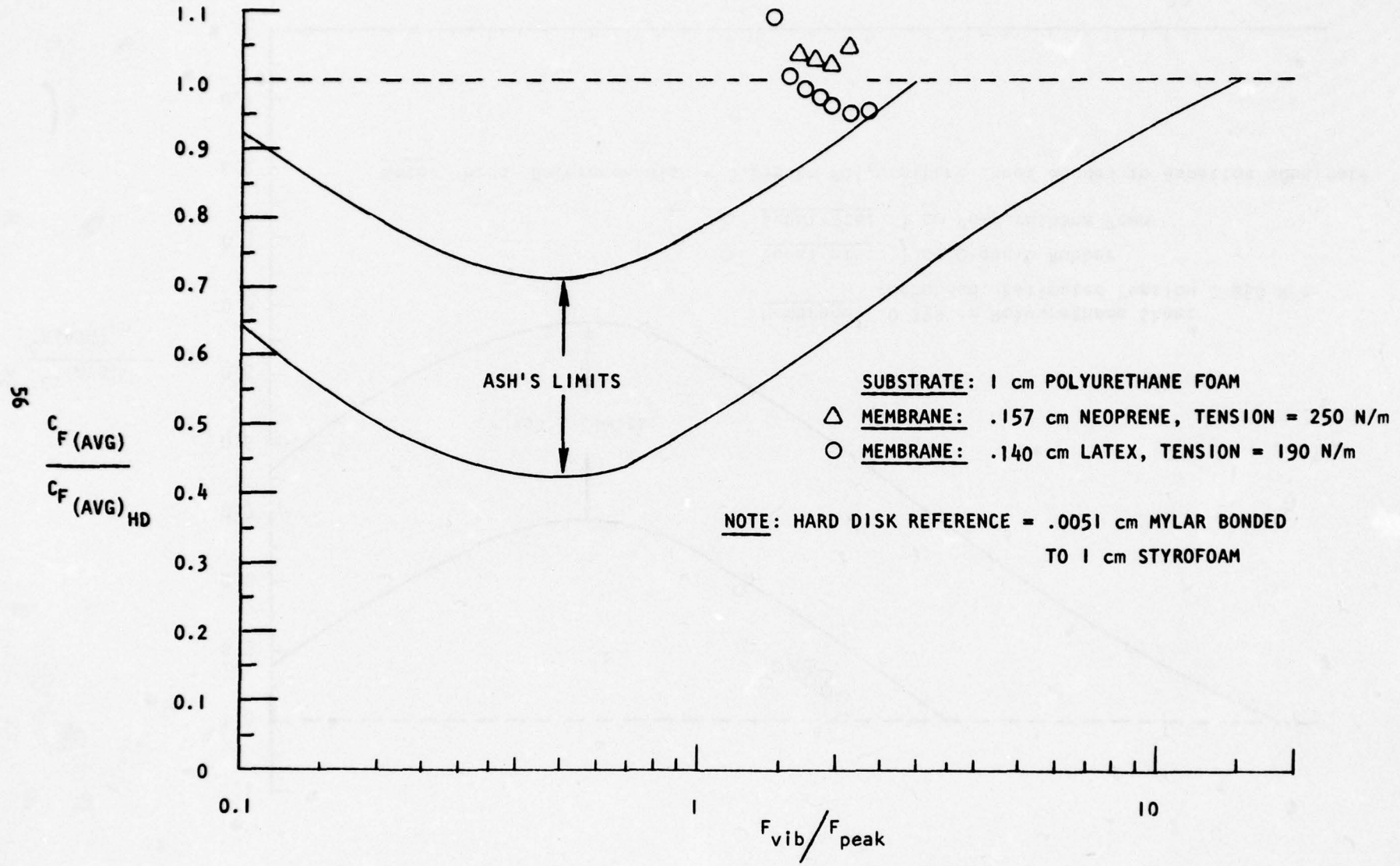

FIGURE 4-22. FREQUENCY DATA FOR DISKS WITH INTERMEDIATE WEIGHT MEMBRANES

Although the frequency ratio has the correct order of magnitude, the latex data indicate an opposite trend with frequency. However, this may simply be due to the formation of standing waves which caused a rapid drag increase with increasing rpm (decreasing F_{vib}/F_{peak}). But the neoprene data clearly suggest there are other variables involved. Thus, Ash's correlation may be a necessary condition but does not appear to be a sufficient condition.

Obvious additional variables are substrate properties and impedance of the water. Water impedance reduces the natural frequency of a membrane. In addition, flexural stiffness is ignored, i.e.,

$$S = \frac{Eh^3}{12(1 - \sigma^2)} \tag{4-6}$$

The corresponding values for the test membranes of polyurethane, neoprene and latex are 0.376 N-cm, 0.0958 N-cm, and 0.0280 N-cm, respectively. Thus measured variations in drag (Figures 4-21 and 4-22) do not show any consistent dependence on stiffness. In the case of plate bending, it can be shown from the appropriate equations of motion that the effects of flexural stiffness increase as frequency increases and wavelength decreases. Therefore, if it is indeed important for a membrane to respond to the high frequencies of turbulence in order to achieve drag reduction,[1] flexural stiffness would be an important variable. Although the limited data presented here cannot be considered conclusive, it does not lend support to this hypothesis.

5.0 CONCLUSIONS AND RECOMMENDATIONS

Based on these compliant disk tests, the following conclusions have been reached.

1. Light weight membranes were not effective in reducing drag. Whereas, heavier membranes appear to be more promising with up to 19% drag reduction. This trend follows Ash's membrane frequency correlation. However, data for disks with heavier membranes also suggest that Ash's correlation may be a necessary condition but is not a sufficient condition.

2. Disk drag was not found to be very sensitive to values of membrane tension greater than 100 N/m. In cases where tension was near zero, standing waves tended to form at low rpm's, and disk drag increased.

3. Bonding a membrane to a given substrate was found to be effective in delaying the formation of standing waves. However, no cases of drag reduction were achieved with this method of assembly. In the cases where drag reduction occurred, the membranes were unbonded in agreement with the flat plate results of Walters[7] and Bushnell et al.[1]

4. The formation of standing waves in a membrane is delayed to higher Reynolds number by increasing Young's modulus of the substrate material. The greatest drag reduction was achieved with organic rubber (CPE) which has a larger Young's modulus than any of the other candidate substrate materials. Thus, the softest substrates are not effective for reducing turbulent skin friction in water.

5. Because of the contribution of vibration to the drag of plastisol disks, small reductions in drag would have been masked. Thus, these spin tests are not considered to be a reliable measure of the drag reducing potential of plastisol substrates.

It is recommended that disks with polyurethane membranes be retested with smooth material. The purpose is to verify the 19% drag reduction which was inferred from data taken with rough polyurethane membranes.

In order to avoid the vibration and flow measurement problems associated with rotating apparatus, it is suggested that a flat plate be used as the basic test surface in future exploratory studies. This would allow detailed flow measurements, and thereby permit a better analysis of the interaction between turbulent, hydrodynamic flows and compliant boundaries. Also, if the effectiveness of polyurethane membranes is verified, this type of compliant boundary should be tested on a flat plate. Although the different geometry may require different membrane thicknesses in order to achieve the desired frequency ratio of one-half. Finally, the comparison of surface properties of successful compliant disks with compliant flat plates may reveal some of the additional key variables.

6.0 REFERENCES

1. Bushnell, D. M., Hefner, J. N., and Ash, R. L., "Compliant Wall Drag Reduction For Turbulent Boundary Layers", IUTAM Symposium on Structure of Turbulence and Drag Reduction, Washington, D. C., June 1976.

2. Offen, G. R. and Kline, S. J., "Combined Dye-Streak and Hydrogen-Bubble Visual Observations of a Turbulent Boundary Layer", Jour. Fluid Mech., Vol. 62, Part 2, 1974.

3. Strickland, J. H. and Simpson, R. L., "Bursting Frequencies Obtained From Wall Shear Stress Fluctuations in a Turbulent Boundary Layer", Physics of Fluids, Vol. 18, No. 3, March 1975.

4. Brown, R. N., "Turbulent Pressure Spectrum Measurements on a Compliant Surface", 4th Biennial Symposium on Turbulence in Liquids, University of Missouri-Rolla, Sept. 1975.

5. Hansen, R. J. and Hunston, D. L., "An Experimental Study of Turbulent Flows Over Compliant Surfaces", Jour. Sound and Vibration, Vol. 34(3), 1974.

6. Hansen, R. J. and Hunston, D. L., "Further Observations on Flow-Generated Surface Waves in Compliant Surfaces", Jour. Sound and Vibration, Vol. 26(4), June 1976.

7. Walters, R. R., "Turbulent Boundary Layer Characteristics of Flow Over a Compliant Surface", Ph.D. Dissertation, University of Oklahoma, 1969.

8. Mattout, R., "Reduction de trainee par parois souples" (Reduction of Drag by Flexible Walls), Association Technique Maritime et Aeronautique, Bulletin No. 72, pp. 207-227, 1972.

9. Weinstein, L. M. and Fischer, M. C., "Experimental Verification of Turbulent Skin Friction Reduction With Compliant Walls", AIAA Jour. Vol. 13, No. 7, July 1975.

10. Ash, R. L., "On The Theory of Compliant Wall Drag Reduction in Turbulent Boundary Layers", NASA CR-2387, April 1974.

11. Goldstein, S., "On the Resistance to the Rotation of a Disc Immersed in a Fluid", Proc. Camb. Phil. Soc., Vol. 31, Part 2, April 1935, pp. 232-241.

12. Theodorsen, T. and Regier, A., "Experiments on Drag of Revolving Disks, Cylinders, and Streamline Rods at High Speeds", NACA Report No. 793, April 1944.

13. Cooper, P., "Turbulent Boundary Layer on a Rotating Disk Calculated With an Effective Viscosity", AIAA Jour., Vol. 9, No. 2., February 1971.

6.0 REFERENCES
(Continued)

14. Granville, P. S., "Torque and Turbulent Boundary Layer of Rotating Disks With Smooth and Rough Surfaces, and in Drag-Reducing Polymer Solutions", Jour. Ship Res., Vol. 17, No. 4, December 1973, pp. 181-195.

15. Fischer, M. C., Weinstein, L. M., Bushnell, D. M., and Ash, R. L., "Compliant Wall Turbulent Skin-Friction Reduction Research", AIAA Paper No. 75-833, June 1975.

16. McLachlan, N. W., Theory of Vibrations, Dover, 1951.

17. Pelt, R. J., "A Preliminary Investigation of Surface Damping Effects on Fluid Flow Through Flexible Tubes", Ph. D. Dissertation, University of Pittsburgh, 1964.

DISTRIBUTION LIST FOR UNCLASSIFIED
TECHNICAL REPORTS ISSUED UNDER
CONTRACT N00014-69-C-0214 TASK NR 062-422

All addresses receive one copy unless otherwise specified

Defense Documentation Center
Cameron Station
Alexandria, VA 22314 — 12 Copies

Technical Library
Naval Ship Research & Dev. Center
Annapolis Laboratory
Anapolis, MD 21402

Professor Bruce Johnson
Engineering Department
Naval Academy
Annapolis, MD 21402

Library
Naval Academy
Annapolis, MD 21402

Professor C. S. Yih
Department of Engineering Mechanics
University of Michigan
Ann Arbor, MI 48108

Professor W. P. Graebel
Department of Engineering Mechanics
University of Michigan
Ann Arbor, MI 48108

Professor T. Francis Ogilvie
Department of Naval Architecture
and Marine Engineering
University of Michigan
Ann Arbor, MI 48108

Professor R. B. Couch
Department of Naval Architecture
and Marine Engineering
University of Michigan
Ann Arbor, MI 48108

Air Force Office of Scientific
Research (REM)
1400 Wilson Boulevard
Arlington, VA 22209

Dr. Coda Pan
Shaker Research Corporation
Northway 10 Executive Park
Ballston Lake, NY 12019

Professor S. Corrsin
Department of Mechanics and
Materials Sciences
The Johns Hopkins University
Charles and 34th Street
Baltimore, MD 21218

Librarian
Department of Naval Architecture
University of California
Berkeley, CA 94720

Professor P. Lieber
Department of Mechanical Engineering
University of California
Berkeley, CA 94720

Professor J. R. Paulling
Department of Naval Architecture
University of California
Berkeley, CA 94720

Professor W. C. Webster
Department of Naval Architecture
University of California
Berkeley, CA 94720

Professor J. V. Wehausen
Department of Naval Architecture
University of California
Berkeley, CA 94720

Professor J. A. Schetz
Department of Aerospace Engineering
Virginia Polytechnic Institute
Blacksburg, VA 24061

Director
Office of Naval Research Branch Office
495 Summer Street
Boston, MA 02210

Commander
Puget Sound Naval Shipyard
Bremerton, WA 98314

Professor G. Birkhoff
Department of Mathematics
Harvard University
Cambridge, MA 02138

Professor G. F. Carrier
Division of Engineering and
Applied Physics
Pierce Hall
Harvard University
Cambridge, MA 02138

Commanding Officer
NROTC Naval Administrative Unit
Massachusetts institute of Technology
Cambridge, MA 02139

Professor M. A. Abkowitz
Department of Ocean Engineering
Massachusetts Institute of Technology
Cambridge, MA 02139

Professor C. C. Mei
Department of Civil Engineering
Massachusetts Institute of Technology
Cambridge, MA 02139

Professor Phillip Mandel
Department of Ocean Engineering
Massachusetts Institute of Technology
Cambridge, MA 02139

Professor E. W. Merrill
Department of Chemical Engineering
Massachusetts Institute of Technology
Cambridge, MA 02139

Professor E. Mollo-Christensen
Department of Meteorology
Room 54-1722
Massachusetts Institute of Technology
Cambridge, MA 02139

Professor J. Nicholas Newman
Department of Ocean Engineering
Room 5-324A
Massachusetts Institute of Technology
Cambridge, MA 02139

Director
Office of Naval Research Branch Office
536 South Clark Street
Chicago, IL 60605

Library
Naval Weapons Center
China Lake, CA 93555

Professor E. Reshotko
Division of Chemical Engineering
Science
Case Western Reserve University
Cleveland, OH 44106

Professor Pai
Institute for Fluid Dynamics and
Applied Mathematics
University of Maryland
College Park, MD 20740

NASA Scientific and Technical Information
Facility
P. O. Box 8757
Baltimore/Washington International Airport
Maryland 21240

Technical Library
Naval Weapons Laboratory
Dahlgren, VA 22418

Dr. C. S. Wells, Jr.
Advanced Technology Center, Inc.
P. O. Box 6144
Dallas, TX 75222

Dr. R. H. Kraichnan
Dublin, NH 03444

Army Research Office
P. O. Box 12211
Research Triangle Park, NC 27709

Dr. Martin H. Bloom
Polytechnic Institute of New York
Department of Aerospace Engineering
and Applied Mechanics
Farmingdale, NY 11735

Technical Documents Center
Army Mobility Equipment R&D Center
Fort Belvoir, VA 22060

Technical Library
Webb Institute of Naval Architecture
Glen Cove, NY 11542

Professor E. V. Lewis
Webb Institute of Naval Architecture
Glen Cove, NY 11542

Dr. M. Poreh
Technion-Israel Institute of Technology
Department of Civil Engineering
Haifa, Israel

Dr. J. P. Breslin
Davidson Laboratory
Stevens Institute of Technology
Castle Point Station
Hoboken, NJ 07030

Mr. C. H. Henry
Stevens Institute of Technology
Davidson Laboratory
Castle Point Station
Hoboken, NJ 07030

Dr. D. Savitsky
Davidson Laboratory
Stevens Institute of Technology
Castle Point Station
Hoboken, NJ 07030

Dr. A. Strumpf
Davidson Laboratory
Stevens Institute of Technology
Castle Point Station
Hoboken, NJ 07030

Dr. J. P. Craven
University of Hawaii
1801 University Avenue
Honolulu, HI 96822

Professor J. F. Kennedy, Director
Institute of Hydraulic Research
University of Iowa
Iowa City, IA 52242

Professor L. Landweber
Institute of Hydraulic Research
University of Iowa
Iowa City, IA 52242

Professor E. L. Resler
Graduate School of Aerospace Engineering
Cornell University
Ithaca, NY 14850

Dr. S. A. Orszag
Flow Research, Inc.
1819 South Central Avenue
Suite 72
Kent, WA 98031

Professor A. T. Ellis
Department of Applied Mathematics and
Engineering Sciences
University of California, San Diego
La Jolla, CA 92037

Dr. J. Young
Science Applications, Incorporated
1250 Prospect Street
La Jolla, CA 92037

Mr. Virgil Johnson, President
Hydronautics, Incorporated
7210 Pindell School Road
Laurel, MD 20810

Mr. M. P. Tulin
Hydronautics, Incorporated
7210 Pindell School Road
Laurel, MD 20810

Commander
Long Beach Naval Shipyard
Long Beach, CA 90801

Professor J. M. Killen
St. Anthony Falls Hydraulic Laboratory
University of Minnesota
Minneapolis, MN 55414

Lorenz G. Straub Library
St. Anthony Falls Hydraulic Laboratory
University of Minnesota
Minneapolis, MN 55414

Professor J. Ripkin
St. Anthony Falls Hydraulic Laboratory
University of Minnesota
Minneapolis, MN 55414

Dr. E. Silberman
St. Anthony Falls Hydraulic Laboratory
University of Minnesota
Minneapolis, MN 55414

Library
Naval Postgraduate School
Monterey, CA 93940

Professor A. B. Metzner
Department of Chemical Engineering
University of Delaware
Newark, DE 19711

Technical Library
Naval Underwater Systems Center
Newport, RI 02840

Office of Naval Research
New York Area Office
715 Broadway - 5th Floor
New York, NY 10003

Professor V. Castelli
Department of Mechanical Engineering
Columbia University
New York, NY 10027

Professor H. G. Elrod
Department of Mechanical Engineering
Columbia University
New York, NY 10027

Engineering Societies Library
345 East 47th Street
New York, NY 10017

Society of Naval Architects and
Marine Engineers
74 Trinity Place
New York, NY 10006

Librarian, Aeronautical Laboratory
National Research Council
Montreal Road
Ottawa 7, Canada

Technical Library
Naval Coastal System Laboratory
Panama City, FL 32401

Dr. J. W. Hoyt
Naval Undersea Center
Code 2501
San Diego, CA 92132

Technical Library
Naval Undersea Center
San Diego, CA 92132

Professor A. J. Acosta
Department of Mechanical Engineering
California Institute of Technology
Pasadena, CA 91109

Professor H. W. Liepmann
Graduate Aeronautical Laboratories
California Institute of Technology
Pasadena, CA 91109

Professor M. S. Plesset
Engineering Science Department
California Institute of Technology
Pasadena, CA 91109

Professor T. Y. Wu
Engineering Science Department
California Institute of Technology
Pasadena, CA 91109

Director
Office of Naval Research Branch Office
1030 E. Green Street
Pasadena, CA 91101

Technical Library
Naval Ship Engineering Center
Philadelphia Division
Philadelphia, PA 19112

Technical Library
Philadelphia Naval Shipyard
Philadelphia PA 19112

Professor R. C. MacCamy
Department of Mathematics
Carnegie Institute of Technology
Pittsburgh, PA 15213

Dr. Paul Kaplan
Oceanics, Inc.
Technical Industrial Park
Plainview, NY 11803

Technical Library
Naval Missile Center
Point Mugu, CA 93041

Commander
Portsmouth Naval Shipyard
Portsmouth, NH 03801

Commander
Norfolk Naval Shipyard
Portsmouth, VA 23709

Dr. H. Norman Abramson
Southwest Research Institute
8500 Culebra Road
San Antonio, TX 78228

Editor
Applied Mechanics Review
Southwest Research Institute
8500 Culebra Road
San Antonio, TX 78206

Dr. Andrew Fabula
Code 5002
Naval Undersea Center
San Diego, CA 92132

Office of Naval Research
San Francisco Area Office
760 Market Street, Room 447
San Francisco, CA 94102

Library
Pearl Harbor Naval Shipyard
Box 400
FPO San Francisco 96610

Technical Library
Hunters Point Naval Shipyard
San Francisco, CA 94135

Professor Bruce H. Adee
Department of Mechanical Engineering
University of Washington
Seattle, WA 98195

Dr. Byrne Perry
Department of Civil Engineering
Stanford University
Stanford, CA 94305

Professor Milton van Dyke
Department of Aeronautical Engineering
Stanford University
Stanford, CA 94305

Professor R. C. DiPrima
Department of Mathematics
Rensselaer Polytechnic Institute
Troy, NY 12181

Professor J. L. Lumley
Department of Aerospace Engineering
Pennsylvania State University
University Park, PA 16802

Professor J. W. Holl
The Pennsylvania State University
Department of Aerospace Engineering
University Park, PA 16801

Dr. J. M. Robertson
Department of Theoretical and
Applied Mechanics
University of Illinois
Urbana, IL 61803

Technical Library
Mare Island Naval Shipyard
Vallejo, CA 94592

Mr. Norman Nilsen (SP 2022)
Strategic Systems Projects Office
Department of the Navy
Washington, D. C. 20376

Office of Naval Research
Code 438
800 N. Quincy Street
Arlington, VA 22217 — 3 Copies

Office of Naval Research
Code 411-6
800 N. Quincy Street
Arlington, VA 22217

Office of Naval Research
Code 412-8
800 N. Quincy Street
Arlington, VA 22217

Office of Naval Research
Code 412-3
800 N. Quincy Street
Arlington, VA 22217

Office of Naval Research
Code 473
800 N. Quincy Street
Arlington, VA 22217

Office of Naval Research
Code 481
800 N. Quincy Street
Arlington, VA 22217

Naval Research Laboratory
Code 2627
Washington, DC 20375 — 6 Copies

Office of Naval Research
Code 1021P (ONRL)
Arlington, VA 22217 — 6 Copies

Naval Research Laboratory
Code 6170
Washington, DC 20375

Naval Research Laboratory
Code 4000
Washington, DC 20375

Naval Research Laboratory
Code 8030
Washington, DC 20375

Naval Research Laboratory
Code 8040
Washington, DC 20362

Naval Sea Systems Command
Code 03C
Washington, DC 20362

Naval Sea Systems Command
Code 0331
Washington, DC 20362

Naval Sea Systems Command
Code 0322 (L. Benen)
Washington, DC 20362

Naval Sea Systems Command
Code 032 (J. Schuler)
Washington, DC 20362

Naval Sea Systems Command
Code 09GS (Library)
Washington, DC 20362

Naval Ship Engineering Center
Code 6034
Center Building
Prince George's Center
Hyattsville, MD 20782

Naval Ship Engineering Center
Code 6101E
Center Building
Prince George's Center
Hyattsville, MD 20782

Naval Ship Engineering Center
Code 6110
Center Building
Prince George's Center
Hyattsville, MD 20782

Naval Ship Engineering Center
Code 6114
Center Building
Prince George's Center
Hyattsville, MD 20782

Naval Ship Engineering Center
Code 6136
Center Building
Prince George's Center
Hyattsville, MD 20782

Dr. A. Powell (Code 01)
David Taylor Naval Ship R&D Center
Bethesda, MD 20084

Mr. W. M. Ellsworth (Code 11)
David Taylor Naval Ship R&D Center
Bethesda, MD 20084

Dr. W. E. Cummins (Code 15)
David Taylor Naval Ship R&D Center
Bethesda, MD 20084

Mr. G. H. Gleissner (Code 18)
David Taylor Naval Ship R&D Center
Bethesda, MD 20084

Mr. R. Wermter (Code 152)
David Taylor Naval Ship R&D Center
Bethesda, MD 20084

Dr. W. B. Morgan (Code 154)
David Taylor Naval Ship R&D Center
Bethesda, MD 20084

Library (Code 5641)
David Taylor Naval Ship R&D Center
Bethesda, MD 20084

Dr. P. Pien (Code 1521)
David Taylor Naval Ship R&D Center
Bethesda, MD 20084

Mr. Paul S. Granville (Code 1541)
David Taylor Naval Ship R&D Center
Bethesda, MD 20084

Mr. J. McCarthy (Code 1552)
David Taylor Naval Ship R&D Center
Bethesda, MD 20084

Dr. Nils Salvesen (Code 1552)
David Taylor Naval Ship R&D Center
Bethesda, MD 20084

Ms. Joanna Schot (Code 1843)
David Taylor Naval Ship R&D Center
Bethesda, MD 20084

Naval Air Systems Command
AIR 03
Washington, DC 20361

Naval Air Systems Command
AIR 5301
Washington, DC 20361

Naval Air Systems Command
AIR 50174
Washington, DC 20361

Naval Sea Systems Command
Code 03B
Washington, DC 20362

Naval Sea Systems Command
Code 03512 (T. Peirce)
Washington, D. C. 20362

Dr. Steven Crow, President
Poseidon Research
15434 Vista Haven Place
Sherman Oaks, California 91403

Strategic Systems Projects Office
Department of the Navy
Washington, DC 20376

Oceanographer of the Navy
200 Stovall Street
Alexandria, VA 22332

Commander
Naval Oceanographic Office
Washington, DC 20373

Dr. A. L. Slafkosky
Scientific Advisor
Commandant of the Marine Corps
(Code AX)
Washington, DC 20380

Librarian Station 5-2
Coast Guard Headquarters
NASSIF Building
400 Seventh Street, S.W.
Washington, DC 20591

Office of Research and Development
Maritime Administration
441 G Street, N.W.
Washington, DC 20235

Division of Ship Design
Maritime Administration
441 G Street, N.W.
Washington, DC 20235

National Science Foundation
Engineering Division
1800 G Street N.W.
Washington, DC 20550

Professor H.-P. Pao
Department of Aerospace & Atmospheric
Sciences
The Catholic University of America
Washington, DC 20017

Dr. G. Kulin
Fluid Mechanics Section
National Bureau of Standards
Washington, DC 20234

Science & Technology Division
Library of Congress
Washington, DC 20540

Chief of Research and Development
Office of Chief of Staff
Department of the Army
Washington, DC 20310

Professor A. Thiruvengadam
Department of Mechanical Engineering
Catholic University of America
Washington, DC 20017

Librarian
Naval Surface Weapons Center
White Oak Laboratory
Silver Sping, MD 20910

Mr. J. Enig (Room 3-252)
Naval Surface Weapons Center
White Oak Laboratory
Silver Spring, MD 20910

Professor J. Wu
College of Marine Studies
Robinson Hall
University of Delaware
Newark, Delaware 19711

Professor V. W. Goldschmidt
School of Mechanical Engineering
Purdue University
Lafayette, Indiana 47907

Professor T. W. Kao
Department of Aerospace & Atmospheric
Sciences
The Catholic University of America
Washington, DC 20017

REPORT DOCUMENTATION PAGE

READ INSTRUCTIONS BEFORE COMPLETING FORM

1. REPORT NUMBER: B-94300/7CR-1
2. GOVT ACCESSION NO.:
3. RECIPIENT'S CATALOG NUMBER:

4. TITLE (and Subtitle): HYDRODYNAMIC DRAG OF DISKS WITH COMPLIANT MEMBRANE/SUBSTRATE FACES.
5. TYPE OF REPORT & PERIOD COVERED: INTERIM rept.,
6. PERFORMING ORG. REPORT NUMBER: B-94300/7CR-1

7. AUTHOR(s): T. D. REED
8. CONTRACT OR GRANT NUMBER(s): N00014-69-C-0214 P00007

9. PERFORMING ORGANIZATION NAME AND ADDRESS:
VOUGHT CORPORATION ADVANCED TECHNOLOGY CENTER, INC.
P. O. BOX 6144, DALLAS, TEXAS 75222

10. PROGRAM ELEMENT, PROJECT, TASK AREA & WORK UNIT NUMBERS:

11. CONTROLLING OFFICE NAME AND ADDRESS:
DEPARTMENT OF THE NAVY
OFFICE OF NAVAL RESEARCH
ARLINGTON, VIRGINIA 22217

12. REPORT DATE: JANUARY 1977
13. NUMBER OF PAGES: 69p.

14. MONITORING AGENCY NAME & ADDRESS(if different from Controlling Office):

15. SECURITY CLASS. (of this report): UNCLASSIFIED
15a. DECLASSIFICATION/DOWNGRADING SCHEDULE:

16. DISTRIBUTION STATEMENT (of this Report)

APPROVED FOR PUBLIC RELEASE; DISTRIBUTION UNLIMITED

17. DISTRIBUTION STATEMENT (of the abstract entered in Block 20, if different from Report)

N/A

18. SUPPLEMENTARY NOTES

N/A

19. KEY WORDS (Continue on reverse side if necessary and identify by block number)

DRAG REDUCTION
COMPLIANT WALL
MEMBRANE WALL
BOUNDARY LAYERS (TURBULENT)
ROTATING DISK
HYDRODYNAMIC FLOWS

10 to the 6th power.

20. ABSTRACT (Continue on reverse side if necessary and identify by block number)

A disk with interchangeable faces of compliant membrane/substrate combinations was spin-tested in a water tank. A device for stretching a membrane uniformly and with repeatable results was designed, fabricated, and successfully employed. Six membrane materials and three substrate materials were utilized to fabricate over 36 different compliant disks. Each of these was tested in turbulent flow over a Reynolds number range of 1.77-2.95 x 10^6. A maximum drag reduction of 19% is indicated from tests with a heavy

(cont on p. 1473B)

389 797

cont'd from p. 14

73 A

polyurethane membrane unbonded to an organic rubber substrate. This amount of drag reduction is inferred from data taken with polyurethane sheet material which had a rough surface finish. Thus, additional tests with smooth polyurethane membranes are needed in order to verify the reported drag reductions ~~reported herein. However, these~~ while the present results tend to follow Ash's membrane frequency criterion, ~~But~~ other data for similar membranes suggest this criterion may be a necessary ~~condition~~ but ~~is~~ not a sufficient condition.

It is recommended that future exploratory studies of the hydrodynamic drag reduction potential of membrane walls be done with flat plates in order to facilitate more detailed flow measurements.

A

1473 B